Transitions to Intermittency and Collective Behavior in Randomly Coupled Map Networks

D. Volchenkov*, S. Sequeira†, Ph. Blanchard,
Zentrum für interdisciplinäre Forschung (ZiF) and
BiBoS and *FSPM - Strukturbildungsprozesse,*
University Bielefeld, Postfach 100131, D-33501, Bielefeld, Germany
and
M.G. Cosenza
Centro de Astrofisica Teórica, Universidad de Los Andes,
A. Postal 26 La Hechicera, Merida 5251, Venezuela

February 8, 2008

Abstract

We study the transition to spatio- temporal intermittency in networks of randomly coupled Chaté-Manneville maps. The relevant parameters are the network connectivity, coupling strength, and the local parameter of the map. We show that spatiotemporal intermittency occurs for some intervals or windows of the values of these parameters. Within the intermittency windows, the system exhibits periodic and other nontrivial collective behaviors. The detailed behavior depends crucially upon the topology of the random graph spanning the network. We present a detailed analysis of the results based on the thermodynamic formalism and random graph theory.

Keywords: *coupled chaotic maps, random graphs, phase transitions, nontrivial collective behavior, spatiotemporal intermittency*
PACS codes: *05.45.+b, 05.70.Fh.*
AMS codes: *82C26, 58F11.*

*dima.volchenkov@uni-bielefeld.de
†sandra@mathematik.uni-bielefeld.de

1 Introduction.

Partial differential equations describing continuous models and real physical systems can, in many cases, be discretized into a system of coupled map lattices (CML). Coupled map lattices are spatiotemporal dynamical systems comprised of an interacting array of discrete-time maps. Much attention to these systems has been drawn in virtue of studies of generic properties of spatiotemporal chaos, [1],[2]. A mean-field extension of CML is the globally coupled map lattice introduced by Kaneko [3]. Here we consider another mean-field extension which refers to random networks of coupled maps.

Although just a few studies devoted to randomly coupled chaotic map networks (RCMN) have been reported by this time, it is beyond dispute that such systems would be very rich in practical applications. To motivate the increasing interest RCMN, one has to note that most real-world networks are of a disordered nature. Social networks [4], biological communities forming food webs [5], and, moreover, computer networks [6], to name just few, have plenty of random shortcuts inconsistent with any regular structure. In this context, interesting investigations of coupled map systems defined on non-uniform lattices have been reported in [7] (CMLs on a Sierpinski gasket) and in [8] (CMLs on a Cayley tree). In view of this, an ensemble of maps coupled at random would provide a forthright model for studying various properties of these disordered networks. The thorough investigation of RCMN would shed new light on the problem of spatiotemporal behavior of discrete extended systems having infinitely many degrees of freedom.

To our knowledge, randomly coupled logistic maps $f(x) = ax(1-x)$ have been considered first in [9]. The emergence of synchronization in random networks of logistic maps with non-local couplings has been investigated in [10], and more recently, dynamical clustering has been observed in maps connected symmetrically at random [11].

We study the collective behavior and phase transitions in a RCMN different from those considered in [9, 11]. The somewhat "statistically simplest" RCMN is considered. On one hand, the Chaté-Manneville map (CM) [12] which we use as a local evolution law can be either in a chaotic or "turbulent" (excited) state, or in a fixed point or "laminar" (inhibited) state. On the other hand, the network topology in our model is spanned by a random graph $\mathbb{G}(N, k)$, corresponding to N sites and such that each site has precisely k outgoing edges.

In the present article, we show that the entire collective behavior is the net result of the interplay between the properties of local map and the probabilistic topology of relevant random graph. Let us note that, in the domain of coupled chaotic maps, the notion of phase transition has been traditionally applied to at least two different classes of phenomena. The first class constitutes the case when a valuable fraction of nodes in the lattice becomes either excited or inhibited at some critical values of the parameters. We shall call these situations either as a transition to intermittency or to relaminarization. The second class refers to the appearance of global periodic motion within a sustained turbulent state. We shall call it as a transition to

collective behavior.

In Sec. 2, the random networks of coupled maps explored in this article are introduced. Section 3 presents the phenomena of spatiotemporal intermittency and nontrivial collective behavior found by direct simulations on randomly coupled Chaté-Manneville maps. In Secs 4, 5, and 6, the observed behavior is analyzed through a theoretical framework. Our approach is twofold. First, we develop a thermodynamic formalism (TD) for RCMN. Secondly, we use the random graph theory invented by P. Erdös and A. Rényi [13], and which has become a basis for discrete mathematics located at the intersection of graph theory, combinatorics, and probability theory [14], [15]. Finally, Sec. 7 contains the conclusions of this work.

2 Coupled maps on random networks.

Let $\Omega \subset \mathbb{Z}$ be the finite lattice of $N \in \mathbb{N}$ sites. At each site $\omega \in \Omega$ there is a local phase space X_ω with an uncountable number of elements. The global phase space $\mathcal{M} = \diamond_{\omega\in\otimes}\mathrm{X}_\omega$ is a direct product of local phase spaces such that a point $\mathrm{x} \in \mathcal{M}$ can be represented as $\mathrm{x} = (x_\omega)$. A *coupled map lattice* is any mapping $\Phi : \mathrm{M} \to \mathrm{M}$ which preserves the product structure, $\Phi\mathrm{x} = (\Phi_\omega x)_{\omega\in\Omega}$, in which $\Phi_\omega : \mathcal{M} \to \mathrm{X}_\omega$. The mapping, $\Phi = G \circ F$, is a composition of an independent local mapping $(Fx)_\omega = f_\omega(x_\omega)$, $f_\omega : \mathrm{X}_\omega \to \mathrm{X}_\omega$, and an interaction, $(Gx)_\omega = g_\omega(x)$.

We consider the following coupled map lattice supplied with some boundary conditions,

$$(\Phi x)_\omega = \left[(1-\varepsilon)\mathbf{I} + \frac{\varepsilon}{k}\mathbf{M}\right] f(x_\omega), \tag{1}$$

where $\varepsilon \in [0,1]$ is the coupling strength parameter, $0 < k < N-1$ is the connectivity number, $\mathbf{I}$ is a unit matrix, and $\mathbf{M}$ is a traceless connectivity matrix, $\mathrm{M}_{jj} = 0$, determining the network topology.

Some models of coupled maps on different random network architectures have been proposed in the literature [9, 10, 11]. Let us note that because of the casuality property, coupled map systems are related to *directed* random graphs. In [9], the connectivity $\mathcal{K}$ is kept fixed, and the connectivity matrix $M_{i,j}$ is not necessary symmetric (if j is a neighbor of i, the reverse may not be true). This random network refers to a *uniform directed random graph*, denoted by $\mathbb{G}(N, \mathcal{K})$ defined on the vertex set $[N]$ with exactly $\mathcal{K}$ edges. Denoting the family of all such graphs as $\mathcal{G}$, we obtain a uniform probability distribution to observe a particular realization $\mathbb{G}(N, \mathcal{K})$,

$$\mathbb{P}(\mathbb{G}) = \left(\begin{array}{c} \left(\begin{array}{c} N \\ 2 \end{array}\right) \\ \mathcal{K} \end{array}\right)^{-1}, \quad \mathbb{G} \in \mathcal{G}$$

.

Two models have been considered in [9]. In the first one, there is a "frozen disorder" with a fixed graph topology configuration. In the second model, new connections are drawn at each time step. From the random graph theory, the second model is known as a random graph *process* $\{\mathbb{G}(N, \mathcal{K})\}_{\mathcal{K}}$ which begins at time 0 and adds new edges, one at a time. The $\mathcal{K}$-th stage

of this Markov process can be identified with the uniform random graph $\mathbb{G}(N,\mathcal{K})$ as it evolves with $\mathcal{K}$ growing from 0 to $\begin{pmatrix} N \\ 2 \end{pmatrix}$.

In [11], the random connectivity matrix is symmetric ($M_{ij} = M_{ij}$), and the matrix elements are either 0 (when the connection between maps i and j is absent) or 1 (if otherwise), while loops are not allowed, ($M_{ii} = 0$). The main advantage of this model is the independent presence of edges, but the drawback is that the number of edges is not fixed, but varies according to a binomial distribution with an expectation $\begin{pmatrix} N \\ 2 \end{pmatrix} p$. This model relies upon a binomial random directed simple symmetric graph, $\mathbb{G}(N,p)$, $0 \leq p \leq 1$.

Another model of a random matrix has been studied in [10]. In this case, the connectivity matrix element M_{ij} is equal to the number of times map i is connected to map j, i.e., possible multiple edges and loops have been taken into account. Therefore, M_{ij} is not necessarily symmetric, and $\sum_i M_{ij} = k$ for any j, i.e. each map is coupled to k maps chosen randomly (it can be coupled to itself). We denote such a random directed graph as $\mathbb{G}^*(N,k)$.

In the present paper, we consider a scheme such that the elements of the connectivity matrix are taken to be either 0 or 1, and the diagonal elements are always taken as 0, i.e. the coupling to itself is ruled out. The number of units in each row of the conectivity matrix is fixed at $k \in [1, N-1]$. Each vertex ω in the relevant random graph has always k outgoing edges. The number of incoming edges is a random Poisson distributed variable with a mean $z = kN/(N-1)$. We denote such a random directed graph as $\mathbb{G}(N,k)$. A random realization of $\mathbb{G}(16,2)$ is given in Fig. (1).

Random graphs $\mathbb{G}(N,1)$ have been extensively studied in [16]-[17]. However, many properties of $\mathbb{G}(N,k)$ for arbitrary k remain to be investigated. A convenient property of such graphs is that they allow an explicit computation of the graph entropy [18] as $h\left(\mathbb{G}(N,k)\right) = \log_2 k$.

Let us note that in the limit $N \to \infty$, the graph $\mathbb{G}(N,k)$ is asymptotically equivalent to $\mathbb{G}^*(N,k)$ considered in [10] since either possibility, that two sites will be connected more than once or that one site will be coupled to itself, are negligible. If $\begin{pmatrix} N \\ 2 \end{pmatrix} p \approx k$, the graph $\mathbb{G}(N,k)$ is also asymptotically equivalent to $\mathbb{G}(N,p)$ (i.e., to a binomial random directed graph). However, it differs substantially from $\mathbb{G}(N,p)$ considered in [11] since we have $M_{ij} \neq M_{ji}$. The properties of $\mathbb{G}(N,k)$, in general, turn out to be quite different from those of either binomial random graphs or uniform random graphs (i.e. having the total number of edges fixed). For example, $\mathbb{G}(N,k)$ are typically sparse but connected.

3 Spatiotemporal intermittency and collective behavior.

Spatiotemporal intermittency in extended systems consists of a sustained regime where coherent and chaotic domains coexist and evolve in space and time. The transition to turbulence via spatiotemporal intermittency has been studied in coupled map lattices whose spatial sup-

ports are Euclidean [9, 19, 20, 21], and also in nonuniform lattices such as fractals [22] and hierarchical lattices [23]. A local map possessing the minimal requirements for observing spatiotemporal intermittency is the Chaté-Manneville map [9]

$$f(x) = \begin{cases} \frac{r}{2}\left(1 - |1 - 2x|\right), & \text{if } x \in [0, 1] \\ x, & \text{if } x > 1, \end{cases} \tag{2}$$

with $r > 2$. This map is chaotic for $f(x)$ in $[0, 1]$. However, for $f(x) > 1$ the iteration is locked on a fixed point. The local state can thus be seen as a continuum of stable "laminar" fixed points ($x > 1$) adjacent to a chaotic repeller or "turbulent" state ($x \in [0, 1]$).

In regular arrays, the turbulent state can propagate through the lattice in time for a large enough coupling, producing sustained regimes of spatiotemporal intermittency [9, 19]. Here, we investigate the phenomenon of transition to turbulence in random networks $\mathbb{G}(N, k)$ using the local map f (Eq.(2)) in the coupled system described by Eq (1). As observed for regular lattices, starting from random initial conditions and after some transient regime, our systems settle in a stationary statistical behavior. The transition to turbulence can be characterized through the average value of the instantaneous fraction of turbulent sites F_t, a quantity that serves as the order parameter [9]. We have calculated $\langle F \rangle$ as a function of the coupling parameter ϵ for several random networks from a time average of the instantaneous turbulent fraction F_t, as

$$\langle F \rangle = \frac{1}{T} \sum_{t=1}^{T} F_t. \tag{3}$$

About 10^4 iterations were discarded before taking the time average in Eq. (3), and T was typically taken at the value 10^4.

We consider Chaté-Manneville maps coupled on a random network $\mathbb{G}(N, k)$ for different parameter values. As initial conditions, we use random cell values uniformly distributed over the interval $[0, r/2]$. Some minimum number of initially excited cells is always required to reach the sustained turbulent state. The typical system size used in the calculations was $N = 10^4$. We have verified that increasing the averaging time T or the network size N do not have appreciable effects on the results.

Two models of random topological configuration have been studied. Model A purposes a random graph to be fixed while the maps are updating. It is, in fact, equivalent to a model of "frozen disorder" proposed in [9]. Model B possesses a random graph which is changed at each time step simultaneously with the updating of the maps.

We have calculated $\langle F \rangle$ vs. ϵ for random networks with different connection numbers k. The local parameter has been kept fixed at $r = 3$ in most of the calculations. Figure (2) shows the mean turbulent fraction $\langle F \rangle$ versus ε for $\mathbb{G}(10^4, 2)$. One can see that, as $\varepsilon > \varepsilon_c \approx 0.145$, the excitation occupies a significant fraction of vertices. The random graph $\mathbb{G}(10^4, 2)$ consists of a set of small disjoint subgraphs of the length ($m \ll N$) and the largest connected component which includes about $O(N^{2/3})$ vertices [15]. The transition to spatiotemporal intermittency for $k = 2$ is characterized by the scaling relation $\langle F \rangle \propto (\varepsilon - \varepsilon_c)^{\beta}$ near the critical value ϵ_c, where

the critical exponent is $\beta = 0.55 \pm 0.03$ for $r = 3$.

A power law behavior of mean turbulent fraction near the onset of spatiotemporal intermittency also occurs for diffusively coupled CM maps in regular Euclidean lattices (i.e., nearest neighbor coupling) [12, 19]. The value of the critical exponent β for the random network with $k = 2$ coincides with that found for the two-dimensional lattice [19, 25].

For $k = 3$, a Hamilton cycle traversing all vertices in the network appears for the first time. There is no isolated vertex in the graph $\mathbb{G}(10^4, 3)$. Fig. (3) shows that the onset of intermittency for the case $k = 3$ occurs more abruptly as k is increased.

Figures (4) and (5) display the mean turbulent fraction $\langle F \rangle$ versus the coupling ε for both Model A and Model B in the RCMN induced by realizations of the random graph $\mathbb{G}(10^4, 4)$. Figs. (4) and (5) show that the onset of intermittency when $k = 4$ occurs as a discontinuous jump in the order parameter $\langle F \rangle$ at the critical value of the coupling. A discontinuous jump of $\langle F \rangle$ at the onset of spatiotemporal intermittency has also been observed for globally coupled Chaté-Manneville maps and interpreted as a first order phase transition in [26].

The error bars shown on $\langle F \rangle$ in Figs. (4) and (5) correspond to the standard deviation (the square root of the variance) of the time series of the instantaneous fraction F_t at each value of ε. With increasing system size N, some of those fluctuations do not fade out. Large, non-statistical fluctuations in the time series of the instantaneous turbulent fraction F_t persist with increasing connectivity k in the networks. For $\varepsilon > 0.5$ these fluctuations appear as large "bulbs" around $\langle F \rangle \approx 1$. This phenomenon is associated to the emergence of nontrivial collective behavior commonly observed in CML systems [27]. In fact, the observed large amplitudes of the standard deviations reflect collective periodic states of the system.

In Figs. (6) and (7) we show the bifurcation diagram of the instantaneous turbulent fraction F_t as a function of the coupling ε for RCMN induced by the random graphs $\mathbb{G}(10^4, 25)$ and $\mathbb{G}(10^4, 30)$, respectively. Figures (6) and (7) reveal a bifurcating band structure for the range of coupling corresponding to the observed large fluctuations in $\langle F \rangle$, reminiscent of the pitchfork bifurcations of unimodal maps.

The return maps at different values of the coupling ε manifest the collective nontrivial behavior in the network. The return maps F_{t+1} vs. F_t for the network $\mathbb{G}(10^4, 25)$ show that before the onset of bifurcations, the sustained turbulent state in the system corresponds to a fixed point with normal statistical fluctuations, as seen in Fig. (8). For $\varepsilon = 0.54$ in Fig. (9), the turbulent fraction shows a period three motion. Other nontrivial collective states can be observed at different parameter values and for random networks with different values of k. For example, Fig. (10) shows that the instantaneous turbulent fraction F_t displays a period-six collective behavior in a RCMN spanned by the random graph $\mathbb{G}(10^4, 30)$ at $\varepsilon = 0.56$ and $r = 3.0$.

For large enough connectivities k, a relaminarization process is observed in the systems. That is, at some $\varepsilon'_c > \varepsilon_c$ the mean turbulent fraction again vanishes, establishing a well defined window of spatiotemporal intermittency. This phenomenon has also been observed in globally

coupled Chaté-Manneville maps [26]. This suggests that the collective properties of randomly coupled map networks and globally coupled maps are similar.

Figure (11) shows $\langle F \rangle$ vs. ε for the RCMN induced by the random graph $\mathbb{G}(10^4, 10)$. The turbulent window is established within the interval $\varepsilon \in [0.33, 0.85]$. Both the forward and backward transitions to the turbulent state appear as discontinuous jumps in the mean turbulent fraction, similar to the windows of turbulence in globally coupled maps [26]. However, for $k > 10$, $\langle F \rangle$ decreases gradually, as shown in Figs. (12) and (13). For connectivities $15 \leq k \leq 40$, the mean turbulent fraction scales as $\langle F \rangle \propto (\varepsilon_c' - \varepsilon)^{-\gamma}$ close to the second critical value ε_c'. The second critical exponent is aproximately the same for different k and was estimated at $\gamma = 0.117 \pm 0.003$, for fixed $r = 3$.

As the connectivity k is increased, the windows of turbulence shrink and eventually disappear, as it can be seen from Figs. (11), (12), and (13). We have plotted the location and the width of the turbulent windows on the coupling parameter axis as a function of the connectivity k for both model A and model B in Figs. (14a) and (14b), respectively. In model A, with frozen connectivity, the turbulent window persists for larger values of k.

4 Probabilistic Geometrical Properties of $\mathbb{G}(N, k)$

In this section, we take the point of view of random graph theory. The reason for this is twofold. First, it leads to the understanding of the threshold phenomena occurring in the transitions to intermittency and relaminarization displayed in the previous section (see Sec. 4.5). Secondly, the knowledge of local structures in a random graph and the counting of its small subgraphs allows us to introduce a notion of *configuration* which is crucially important for the thermodynamic formalism applied to the chaotic coupled maps defined on a random graph (see Sec. 5).

The observations reported in [9] and [11] indicate that the detailed evolution of dynamical clustering depends crucially on the entire architecture of the particular network. To define the probabilistic geometrical properties of a random graph, one has to chose a certain procedure of random graph generation, i.e. a *configuration model*. There is a number of constructive procedures asymptotically almost surely (*a.a.s.*) leading to $\mathbb{G}(N, k)$. In most cases, however, these constructions do not give a uniformly distributed random graph, but it can be checked out if the relevant distributions are contiguous to a uniform one [15]. In this paper, we follow the configuration model proposed first in [14], and which leads to a uniform distribution of graphs.

Let $N, k \in \mathbb{N}$ be such that kN is even and $k \leq N - 1$. The vertex set of a graph is $\Omega = [N]$. It is natural to define the "*in*-" and "*out*"-components separately for each vertex as the sets of vertices which can either be reached or reacheable from a given vertex $\omega \in \Omega$. Let us arrange that the in-component $\mathcal{I}_t(\omega) \subset \Omega$ is a set of vertices which are coupled to a given vertex ω in Eq. (1) at time t. Consequently, we shall name a set of vertices to which the vertex ω is coupled

in Eq. (1) at time $t+1$ as the out-component $\mathcal{O}_t(\omega) \subset \Omega$.

4.1 The structure of in-components

If the connectivity k is fixed, the incoming degree $s_i = |\mathcal{I}_t(\omega_i)|$ of the vertex ω_i in a random graph is a random variable distributed in accordance with the Poisson distribution $\mathrm{Po}(z) = z^n e^{-z}/n!$, where $z = kN/(N-1)$ is the average number of incoming links [15], [28]. With respect to the backward time direction, the properties of $\mathbb{G}(N,k)$ are equivalent to those of a uniform directed random graph $\mathbb{G}(N, kN/2)$.

If k is small and independent of N, *a.a.s* all components of $\mathbb{G}(N, kN/2)$ are trees or unicyclic, the largest of which have $O(\log N)$ vertices. As the connectivity approaches $k=2$, very quickly all the largest components merge into one giant component roughly of $O(N^{2/3})$ vertices (see Fig. 1). The size distribution of remaining small clusters behaves as $P_\mu \propto \mu^{-3/2}\exp(-\mu)$ [28]. Then, another jump in the size of giant component occurs from $O(N^{2/3})$ to roughly $O(N)$. This phenomenon of a "double jump" in the evolution of $\mathbb{G}(N, cN)$ was firstly discussed in [29].

Note that the appearance of the giant component at $k=2$ however, does not guarantee that there are no isolated vertices in the graph, and that each vertex can be reachable from a given one. In fact, as $k=2$, the random graph consists of a number of small disjoint clusters of sizes $m \ll N$.

4.2 The configuration model and subgraphs classification

Next we study the graph following the forward traversal of edges that corresponds to the natural (forward) lapse of time. In the constructive procedure, we associate the disjoint k-element sets $\mathcal{O}_t(\omega)$ to each element $\omega \in \Omega$ such that $\mathbb{W}_t = \Omega \times \mathcal{O}_t(\omega)$. The points in $\mathbb{W}_t$ are the outgoing tails, $|\mathbb{W}| = (kN-1)!! = (kN)!/2^{kN/2}(kN/2)!$. Then, a configuration Θ_t is a partition of $\mathbb{W}_t$ into $kN/2$ directed pairs which we call the outgoing edges. The natural projection $\Pi_t : \mathbb{W}_t \to \Omega$ projects each configuration Θ_t to a directed multigraph $\pi(\Theta_t)$. If $\pi(\Theta_t)$ lacks loops and multiple edges, it is equivalent $\mathbb{G}(N,k)$.

One should note that if the latter condition on $\pi(\Theta_t)$ being a simple graph is omitted, we arrive at the model $\mathbb{G}^*(N,k)$ discussed in [10]. The crucial point concerning to $\mathbb{G}^*(N,k)$ is that it does not have a uniform distribution over all multigraphs on Ω since different multigraphs arise from different numbers of configurations (yielding the additional factors of $1/2$ for each loop and $1/m!$ for each edge of multiplicity m). Nevertheless, as $N \to \infty$ any property that holds *a.a.s* for $\mathbb{G}^*(N,k)$ also holds *a.a.s* for $\mathbb{G}(N,k)$.

With respect to the forward traversal of edges, the random graphs appearing in the above procedure are the k-regular directed random graphs. A cursory observation of Fig. 1 convinces one that such a graph comprises of a set of typical subgraphs. A standard ground for their classification is given by an *excess* [15]. A component $\mathcal{H}$ of a graph is an *ℓ-component* if it has $K>0$ vertices and $K+\ell$ edges, where ℓ is the excess of $\mathcal{H}$. Note that for any connected

component $\ell \geq -1$. $\ell = -1$ only for tree like components that is a finite sequence of edges (ω_i, ω_{i+1}) such that $\mathcal{O}_t(\omega_i) = \mathcal{I}_t(\omega_{i+1})$ for $1 \leq i \leq m-1$, where m is a *length* of the path.

Each $0-$component is unicyclic, i.e. a path that starts and terminates at the same vertex. Other complex $\ell-$components with $\ell > 0$ contains at least two simple sub-cycles.

4.3 The counting of small subgraphs and configuration

Let $k = |\mathcal{O}_t(\omega)|$ and $N = [\Omega]$. Directly from definitions it follows that the probability to observe any given set of m disjoint directed edges on $\mathbb{W}$ in a random configuration reads as [15],

$$p_m = \frac{(kN-2m-1)!!}{(kN-1)!!}. \tag{4}$$

Let us note that if m is fixed, this probability shows a power law behavior

$$p_m \sim_{N\to\infty} (kN)^{-m}, \tag{5}$$

otherwise,

$$p_m \sim_{kN-m\to\infty} \left(\frac{e}{N}\right)^m \left(k - \frac{2m}{N}\right)^{kN/2-m} k^{-kN/2}. \tag{6}$$

The latter relation follows from (4), the expression $(n-1)!! = \sqrt{2}n^{n/2}e^{-n/2}(1 + \mathrm{O}(1/n))$, and the Stirling formula.

Let us count the number X_m^ℓ of various small ℓ-components of the length m (here, 'small' means $m \leq N-1$) appearing in $\mathbb{G}(N,k)$. Note that $X_m^{\ell>m-1} \equiv 0$, and $X_1^0 = 0$ is the number of loops. Therefore, X_2^0 is the number of simple directed two-vertex cycles, X_3^0 is the number of directed triangles, etc. As $N \to \infty$ in a random graph, X_m^ℓ are the random variables such that their distributions converge jointly in $\mathbb{R}^\infty$ to the Poisson distributions $\mathrm{Po}(\lambda_k^\ell)$, where $\lambda_k^\ell = \mathbb{E}X_m^\ell$ are the expectations of X_m^ℓ [15].

The number of directed path ($\ell = -1$) of length m can be calculated readily, $\mathrm{Pa}_m = (N)_m k^m \prod_{i=2}^m s_i \simeq N^m k^m \prod_{i=2}^m s_i$, in which $(N)_m$ is the falling factorial [30] and s_i is the incoming degree of the vertex ω_i . Remember that s_i is a random variable having a distribution contiguous to the Poisson one. Then, $\lambda_m^{(-1)} = \mathbb{E}X_m^{(-1)} = p_m \mathrm{Pa}_m = \prod_{i=2}^m s_i \sim z^{m-1} = k^{m-1}$ as $N \to \infty$.

Analogously, for the number of simple cycles, one obtains $\lambda_m^0 = m^{-1} \prod_{i=1}^m s_i \sim_{N\to\infty} m^{-1} \times (k)^m$, in which the factor $1/m$ comes from all permutations of vertex indices within the cycle. Then, for the number of 1-component subgraphs, we arrive at $\lambda_m^1 = (m-2)^{-1}(k-1)^m \prod_{i=1}^m s_i \times \prod_{j=1}^{m-1}(s_j - 1) \sim_{N\to\infty} k^m(k-1)^m(k-2)^{m-1}/(m-2)$ and so on.

Due to properties of the Poisson distribution, one obtains the following asymptotic relation for the factorial moments (i.e. the number of ordered pairs $(X_m^\ell)_2$, triplets $(X_m^\ell)_3$, quadruplets $(X_m^\ell)_4$, etc.)

$$(X_{m_1}^\ell)_{i_1}(X_{m_2}^\ell)_{i_2}\dots(X_{m_n}^\ell)_{i_n} \longrightarrow_{N\to\infty} (\lambda_{m_1}^\ell)^{i_1}(\lambda_{m_2}^\ell)^{i_2}\dots(\lambda_{m_n}^\ell)^{i_n}. \tag{7}$$

A set of pairs $\Theta(\mathbb{G}) = \left\{m, X_m^\ell\right\}_{\ell=-1}^{m-1}$ is the *configuration* of a graph $\mathbb{G}$.

4.4 Hamilton Cycles and Perfect Matching

Hamilton cycles H are the directed cycles of length N. The analysis developed in the previous subsection gives for the expectation number of cycles $m = N$,

$$\mathbb{E}H_k = (N-1)!\frac{(kN-2N-1)!!}{(kN-1)!!} \cdot k^N \prod_{i=1}^{N} s_i. \tag{8}$$

If $k = 0$ or 1, then there is no Hamilton cycles in $\mathbb{G}(N,k)$. If $k = 2$ Eq. (8) yields

$$\mathbb{E}H_2 = \frac{(N-1)!}{(2N-1)!!} \sim_{N\to\infty} \sqrt{\frac{\pi}{N}} \longrightarrow_{N\to\infty} 0. \tag{9}$$

Hence there is also *a.a.s* no Hamilton cycles in $\mathbb{G}(N,2)$.

As $k \geq 3$, the number of Hamilton cycles in $\mathbb{G}(N,k)$ exhibits a threshold. Namely, in

$$\mathbb{E}H_{k\geq 3} \sim_{N\to\infty} \sqrt{\frac{\pi}{2N}} \left[\frac{(k-2)^{k/2-1}}{k^{k/2-2}}\right]^N \tag{10}$$

the quantity within the square brackets is greater than 1 for any $k \geq 3$, therefore, $\mathbb{E}H_{k\geq 3} \to \infty$ as $N \to \infty$. Therefore, $\mathbb{G}(N,k)$ has lots of Hamiltonian cycles when $k \geq 3$. As a matter of fact, it means that $\mathbb{G}(N,k)$ has no isolated vertices as $k \geq 3$, i.e. there is a perfect matching which covers every vertex of the graph.

The case of $k = 4$ is of a particular interest since the number of edges $e = 2N$, i.e. the excess is $\ell = N$. Here we refer to a result of [15] (see also references therein) about the contiguity of probability distributions defined on a simple sum of two Hamilton cycles $\mathbb{H}(N)$ and the random graph $\mathbb{G}(N,4)$,

$$\mathbb{H}(N) + \mathbb{H}(N) \asymp \mathbb{G}(N,4). \tag{11}$$

The latter statement means that, as $N \to \infty$, the probability measures defined on $\mathbb{G}(N,4)$ and on two independent Hamilton cycles $\mathbb{H}(N) + \mathbb{H}(N)$ are mutually absolutely continuous.

4.5 Sharp and coarse thresholds in RCMN

In the Sec. 3, we have encountered a number of threshold phenomena related to transitions to intermittency and backward to a laminar state. At the onset of intermittency, i.e. as $\varepsilon \to \varepsilon_c-$ and r fixed, there is a monotone increasing property of $\mathbb{G}(N,k)$ to have an induced turbulent subgraph G which calls for a close attention. Similarly, as $\varepsilon \to \varepsilon_c'-$, for r fixed, one can define a monotone decreasing property of having a laminar subgraph.

We define the intermittency threshold for the RCMN $\mathbb{G}(N,k)$ as follows. Let us suppose that there are F_tN excited cells in Ω at time t. Consider a subgraph $G \subseteq \mathbb{G}(N,k)$ such that the vertex set $[F_tN]$ of G is $[F_tN] \subseteq [N]$ and the edge set $E[G] = E[\mathbb{G}(N,k)] \cap (F_tN)^2$. We shall call G as the *induced turbulent subgraph* of the random graph $\mathbb{G}(N,k)$.

Directly from Eqs. (1) and (2) one obtains that a site ω that is laminar at time t becomes turbulent at time $(t+1)$ if $x_\omega(t) \in [1, x_m(\omega;t)]$ where $x_m(\omega;t)$ is the maximum value that a

laminar cell may have in order to become turbulent in the next iteration,

$$x_m(\omega;t) = \frac{1-\varepsilon\varphi(\omega;t)}{1-\varepsilon},$$

where $\varphi(\omega;t) = s_\omega^{-1}\sum_{\omega'\in\mathcal{I}_t(\omega)} f\left(x_{\omega'}(t)\right)$. Therefore, $P\{1\leq x_\omega(t) < x_m(\omega;t)\}$ is the probability that ω becomes turbulent at the next time step. Consequently, $P\{x_m(\omega;t)/r < x_\omega(t) < 1 - x_m(\omega;t)/r\}$ is the probability that the cell ω being turbulent at time t becomes laminar at time $t+1$.

Let us denote a sequence of probabilities that the site ω is turbulent at time $t+1$ at different values of coupling ε as

$$\mathfrak{p}(\varepsilon) = P\{1\leq x_\omega(t) < x_m(\omega;t)\}$$
$$\times\left(1 - P\{x_m(\omega;t)/r < x_\omega(t) < 1 - x_m(\omega;t)/r\}\right).$$

Then we define a limit $\mathfrak{p}_c = \lim_{\varepsilon\to\varepsilon_c}\mathfrak{p}(\varepsilon)$. For an increasing property of having the induced turbulent subgraph $G\subseteq\mathbb{G}(N,k)$, a sequence $\mathfrak{p}(\varepsilon)$ is called a *threshold* if

$$\mathbb{P}\left\{G\subseteq\mathbb{G}(N,k)\right\} = \begin{cases} 0, & \mathfrak{p}(\varepsilon)\ll\mathfrak{p}_c \\ 1, & \mathfrak{p}(\varepsilon)\gg\mathfrak{p}_c. \end{cases} \tag{12}$$

Furthermore, $\mathfrak{p}_c$ is called a *sharp* threshold if for every $\eta > 0$, $\mathbb{P}\left\{G\subseteq\mathbb{G}(N,k)\right\} = 0$ as $\mathfrak{p}\leq(1-\eta)\mathfrak{p}_c$, and $\mathbb{P}\left\{G\subseteq\mathbb{G}(N,k)\right\} = 1$ as $\mathfrak{p}\geq(1-\eta)\mathfrak{p}_c$, otherwise we shall call $\mathfrak{p}_c$ as a *coarse* threshold.

A recent result [31] establishes that graph properties that depend on the inclusion of a large subgraph have always sharp thresholds. A monotone graph property with a coarse threshold may be approximated by the property of containing at least one of a certain finite family of small graphs as a subgraph. This statement gives us a key to understanding the nature of the transitions to intermittency occurring in RCMN.

Indeed, as $k=2$, the random graph $\mathbb{G}(N,k)$ consists of merely small subgraphs. Some of them become turbulent as $\varepsilon\geq\varepsilon_c$, establishing a coarse threshold. If $k\geq 3$, the random graph $\mathbb{G}(N,k)$ is connected; moreover, it comprises of a number of Hamilton cycles, and consequently, the intermittency threshold is sharp. Otherwise, if the connectivity is around $k=10$, the relaminarization process which starts as $\varepsilon\to\varepsilon_c'-$ appears as a sharp threshold since, probably, a whole Hamilton cycle becomes laminar at once. However, for k substantially greater than 10, the relaminarization process comes step by step over small subgraphs establishing a coarse threshold.

We conclude this section with a note on a power law for a monotone graph property close to a threshold value. For a coarse threshold, there are $n\in\mathbb{N}$ and $\alpha\in\mathbb{R}$ such that $\mathfrak{p}(\varepsilon,t)\asymp n^{-\alpha}$. More precisely, there is a partition of $[N]$ into a finite number of sequences $[N_1],[N_2],\ldots[N_m]$ (i.e., induced subgraphs) and rational numbers $\alpha_1,\alpha_2,\ldots\alpha_m > 0$ such that $\mathfrak{p}(\varepsilon,t)\asymp n_j^{-\alpha_j}$ for $n_j\in[N_j]$, [15].

5 Thermodynamic Formalism for Coupled Maps on Random Networks

In this section, we consider the thermodynamic formalism (TD) approach to the behavior of coupled maps defined on random networks. TD relies upon a symbolic representation for the coupled maps dynamics. The general idea of the approach is to study this representation via Gibbs states for the $(d+1)$-dimensional system which goes back to [32] and [33].

5.1 The formal definition of randomly coupled map networks.

We give a rigorous definition for ensembles of coupled maps defined on a random graph. Consider a finite set $\Xi \subset \mathbb{Z}$ such that $|\Xi| = \mathcal{N} < \infty$ and $k \in \mathbb{Z}_+,\ \ k \leq \mathcal{N} - 1$, such that $k\mathcal{N}$ is even. Following the standard configuration model (Sec. 4.2), one associates the disjoint $k-$element sets $\mathcal{O}_t(\upsilon)$ to each element $\upsilon \in \Xi$. As a result, one arrives at the set of outgoing tails $\mathbb{W}_t = \Xi \times \mathcal{O}_t(\upsilon)$. A partition Θ_t of $\mathbb{W}_t$ into $k\mathcal{N}/2$ directed pairs which we call the outgoing edges. Then the natural projection $\pi\left(\Theta_t(\mathbb{G})\right)$ is a simple random graph $\mathbb{G}(\mathcal{N}, k)$.

At each node $\varpi \in \Xi$, we define a local phase space X_ϖ with an uncountable number of elements. The global phase space $\mathrm{M}_{\mathbb{G}(\mathcal{N},k)} = \Pi_{\varpi\in\Xi}\mathrm{X}_\varpi$ is a direct product of local phase spaces such that a point $\mathrm{x} \in \mathrm{M}_{\mathbb{G}(\mathcal{N},k)}$ can be represented as $\mathrm{x} = (x_\varpi),\ \ \varpi \in \Xi$.

Let us suppose that there is a subset $\Omega \subset \Xi$ such that $|\Omega| = N \ll \mathcal{N}$. Consider a subgraph $\mathbb{G}(N,k) \subset \mathbb{G}(\mathcal{N},k)$ such that the edge set $E\left[\mathbb{G}(N,k)\right] = E\left[\mathbb{G}(\mathcal{N},k)\right] \cap \Omega^2$. Then $\mathbb{G}(N,k)$ is a random graph *induced* by Ω. For each $\omega \in \Omega$, we denote the local phase space $\mathrm{X}_\omega \subseteq \mathrm{X}_\varpi$, and the global phase space $\mathrm{M}_{\mathbb{G}(N,k)} = \Pi_{\omega\in\Omega}\mathrm{X}_\omega$ such that $\mathrm{M}_{\mathbb{G}(N,k)} \subseteq \mathrm{M}_{\mathbb{G}(\mathcal{N},k)}$. In what follows, we denote $\mathrm{M}_{\mathbb{G}(N,k)}$ simply as $\mathrm{M}_\mathbb{G}$ and take the limit $\mathcal{N} \to \infty$.

The *randomly coupled map network* (RCMN) defined on the random graph $\mathbb{G}(N,k)$ is a mapping $\Phi_\mathbb{G} : \mathrm{M}_\mathbb{G} \to \mathrm{M}_\mathbb{G}$ which preserves the product structure, $\Phi_\mathbb{G}\mathrm{x} = (\Phi_\omega x)_{\omega\in\Omega}$, such that $\Phi_\omega : \mathrm{M}_\mathbb{G} \to \mathrm{X}_\omega$.

As usual, the mapping $\Phi_\mathbb{G} = C \circ F$, can be considered as a composition of the local mapping $(Fx)_\omega = f_\omega(x_\omega)$, which is independent from the graph topology, $f_\omega : \mathrm{X}_\omega \to \mathrm{X}_\omega$, and the interaction $(C_\mathbb{G}x)_\omega = g_\omega^\mathbb{G}(x)$.

In the framework of thermodynamic formalism, we seek for a symbolic representation for the dynamic of the coupled map system $(\Phi_\mathbb{G}x)_\omega,\ \ \omega \in \Omega$ on the cylinder $\mathbb{L} = \Omega \times \mathbb{Z}_+$ where $\Omega \subset \Xi$. Regarding the above definition, models A and B introduced before can be considered. In Model A, there is the "frozen disorder" proposed first in [9], where the configuration $\Theta(\mathbb{G})$ is kept fixed while the map Φ is iterating. In Model B, the configuration $\Theta_t(\mathbb{G})$ is changed at each time step as the map is updated.

Let us note that from the definition of RCMN given above, in the limit $\mathcal{N} \to \infty$ both Model A and Model B are not very different. The numbers of small subgraphs $X_m^\ell(\mathcal{N})$ in the entire random graph $\mathbb{G}(\mathcal{N},k)$ are random variables fluctuating about their expectation values λ_m^ℓ. Let us define a discrete time *random graph process* $\{\mathbb{G}(\mathcal{N},k)\}_\mathcal{N}$ which describes the growth of

the entire random graph $\mathbb{G}(\mathcal{N},k)$ as $\mathcal{N}\to\infty$. This is obviously a Markov process with time running through the discrete set $\{0,1,\dots k\mathcal{N}/2\}$. Hence, one has $t=O(\mathcal{N})$ as $\mathcal{N}\to\infty$.

The graph $\mathbb{G}(N,k)$ is a small subgraph of $\mathbb{G}(\mathcal{N},k)$ induced by $\Omega\subset\Xi$. The configuration of $\mathbb{G}(N,k)$ also varies as $\mathcal{N}$ grows. The numbers of small subgraphs $X_m^\ell(\mathcal{N},N)\simeq X_m^\ell(t,N)$ are the Poisson distributed random variables (since $\mathbb{E}(X_m^\ell)_k=(\lambda_m^\ell)^k$) such that $X_m^\ell(t,N)\longrightarrow\lambda_m^\ell$ as $t\to\infty$ and $N\to\infty$. Therefore, even in the model of "frozen disorder", Model A, the actual configurations would change at each time step.

5.2 Symbolic dynamics and Gibbs states for the RCMN

Given the configuration of the entire random graph $\Theta_{\mathcal{N}}=\pi^{-1}\left(\mathbb{G}(\mathcal{N},k)\right)$, a symbolic dynamics is defined as a direct product $\mathcal{T}=\pi^{-1}\otimes T$, where T is a semi-conjugacy (since, in principle, there would be no inverse map on the partition boundaries) to the map Φ on $M_{\mathbb{G}}$ from a subshift σ on a symbolic configuration space M_Φ^s:

$$\forall\xi\in M_\Phi^s,\quad T(\sigma\xi)=\Phi T(\xi),\tag{13}$$

and π^{-1} is conjugated to a subshift τ on a random graph configuration space $\mathbb{W}$,

$$\pi^{-1}(\tau\Theta_{\mathcal{N}})=\pi^{-1}(\Theta_{\mathcal{N}+1}).\tag{14}$$

Relations (13)-(14) purport a Markov partition $\mathcal{V}_{\xi,\Theta}$ to be defined with an index set $M_{\mathbb{G}}^s=A^s$ for a finite alphabet A. The simplest possible alphabet would comprise just of two letters, $A=\{0,1\}$, indicating either "excited" or "inhibited" state.

As a result, to any spatio-temporal configuration $x\in M_{\mathbb{G}}:x=(x_\varpi),\varpi\in\Xi$, a symbolic code $\xi=(\xi_t),t\in\mathbb{Z}_+$ is assigned, and $M_{\Phi,\mathbb{G}}^s$ is the set of all such codes.

The thermodynamic formalism comes about by asking for a conditional probability distribution on symbolic configurations defined on a cylinder $\mathbb{L}=\Omega\times\mathbb{Z}_+,\ \Omega\subset\Xi$, given a symbolic configuration on the complement $\mathbb{L}^c=\Omega^c\times\mathbb{Z}_+,\ \Omega^c=\mathbb{Z}\setminus\Omega$. On the uniformly hyperbolic subsets $K\subseteq M_{\mathbb{G}}$ these conditional probabilities are given by the Gibbs states,

$$P\left(\xi_{\mathbb{L}}|\,\xi_{\mathbb{L}^c}\right)=Z^{-1}\exp\left[-\mathcal{F}_{\mathbb{L}}(\xi)\right],\tag{15}$$

where $\mathcal{F}_{\mathbb{L}}(\xi),\ \ (\xi_t)_\omega\in M_{\Phi,\mathbb{G}}^s,\ \ (\omega,t)\in\mathbb{L}$ is a part of the potential

$$\mathcal{F}(\xi,\Theta)=\sum_{t\in\mathbb{Z}_+}\log\left|\det[D^{(u)}\Phi]\left(\mathcal{T}(\sigma^t\xi,\tau^t\Theta)_{(\varpi,t)}\right)\right|,\tag{16}$$

which plays the role of a Hamiltonian in statistical mechanics. The Jacobian matrix $[D^{(u)}\Phi]$ is restricted to a unstable subspace which is the whole tangent space $TM_{\mathbb{G}}$ for expanding maps, $N\to\infty$. We shall drop the index (u) in the sequel.

The normalization factor Z in (15) is a partition function,

$$Z=\sum_{\eta\in M_{\Phi,\mathbb{G}}^s}\exp\left[-\beta\mathcal{F}(\eta)\right],\tag{17}$$

where the sum in (17) is performed over all configurations $\eta \in M^{\mathrm{s}}_{\Phi,\mathbb{G}}$ which coincide with ξ on $\mathbb{L}$.

Although, in general, the feasibility of introducing the thermodynamic formalism defined in Eqs.(15)-(17) for a coupled map lattice in any dimension and for any values of the coupling strength $\varepsilon > 0$ could be questionable, nevertheless, for a 1D piece-wise linear map this approach is indeed always possible [34].

6 Transitions to Intermittency and Collective Behavior in the RCMN

All information on transitions to intermittency and collective behavior in the RCMN is contained in the Gibbs potential $\mathcal{F}$ (16). In statistical mechanics it is somewhat unusual because, even in the uncoupled case, the Gibbs potential has nontrivial interactions in the time direction [35], [36]. However, a formal analogy between transitions to spatiotemporal intermittency observed in the RCMN and phase transitions in uniaxial ferromagnets can be found.

For the coupled map system (1)-(2), the potential $\mathcal{F}$ is a function of three external parameters, $\{\varepsilon, r, k\}$. The hyperbolicity of phase space means a positivity of all Liapunov exponents in the spectrum, $\lambda_n > 0$. From direct numerical simulations, it is known that the number of positive Liapunov exponents for extended chaotic systems scales as the lattice size [37], $N_{\lambda_n>0} \sim N$. This means that in the extended limit $N \to \infty$ the instantaneous turbulent fraction $F_t = N_{\mathcal{T}}(t)/N$ is a natural order parameter monitoring the transition to intermittency in a coupled chaotic map system.

Since the matrix element of $[D\Phi]$ in (16) relevant to a site ϖ being in the turbulent state is proportional to r, the instantaneous turbulent fraction can be simply counted as

$$F_t = -\frac{\partial \mathcal{F}(r, \varepsilon, k)}{\partial r}. \tag{18}$$

The analogy with the uniaxial ferromagnet is the following. Let us assign the turbulent state to a "spin up" configuration and the laminar state to a "spin down". Then F_t is a spontaneous magnetization in the ferromagnet with the interaction Hamiltonian (16). The mean turbulent fraction

$$\langle F \rangle = \frac{\partial \log Z}{\partial r}, \tag{19}$$

in which Z is the partition function (17), is equivalent to the magnetization in the ferromagnet.

Carrying on this analogy, one can introduce the Gibbs free energy function $\mathcal{U}$ for the system of coupled chaotic maps. Let us define a finite piece $\mathbb{L}_{\mathcal{N}} \subset \mathbb{L}$ of the cylinder $\mathbb{L} = \Omega \times \mathbb{Z}_+$ having a volume $\mathbb{V}_{\mathcal{N}} = N \cdot c\mathcal{N}$ where $c < \infty$. One can introduce a restriction $\mathcal{F}_{\mathbb{L}_{\mathcal{N}}}$ of the potential $\mathcal{F}_{\mathbb{L}}$ on the finite cylinder $\mathbb{L}_{\mathcal{N}}$. Then the free energy is $\mathcal{U} = \lim_{\mathcal{N}\to\infty} \mathcal{F}_{\mathcal{N}}/\mathbb{V}_{\mathcal{N}}$.

6.1 The equation for the free energy function

Following [35], [36], and [38], we now apply a simple transformation to (16). We use the standard relation log det = Tr log which gives us the following expression for the Gibbs potential

$$\mathcal{F}_{\mathbb{L}}(\xi|_{\mathbb{L}}, \Theta) = \sum_{t\in\mathbb{Z}_+} \mathrm{Tr}\left(\log|[D\Phi]|\right)_{\omega,\omega}\left(\mathcal{T}(\sigma^t\xi, \tau^t\Theta)_{(\omega,t)}\right), \quad (\omega, t) \in \mathbb{L}. \tag{20}$$

Since the local map (2)is 1D, then $\log D\Phi_\omega$ can be defined as the number $\log|D\Phi_\omega|$. The notation $(\log|[D\Phi]|)_{\omega,\omega}$ indicates the diagonal block corresponding to site $\omega \in \Omega$. The trace is summed over the whole induced subgraph $\mathbb{G}(N, k) \subset \mathbb{G}(\mathcal{N}, k)$ and is independent of any choices.

Returning to the map Eqs. (1)-(2), one can proceed further using the potential (20). The Jacobian matrix in (20) can be written in the form $[D\Phi] = \mathbb{U}(\mathbb{I} - \mathbb{U}^{-1}\mathbb{C})$, where $\mathbb{U}$ is a contribution coming from the *uncoupled* maps (i.e., the diagonal part of $[D\Phi]$), and $\mathbb{C}$ comes from the coupling. Then we expand $\mathrm{Tr}\log|[D\Phi]| = \mathrm{Tr}\log|\mathbb{U}| - \sum_{s>0}\mathrm{Tr}\left[(\mathbb{U}^{-1}\mathbb{C})^s/s\right].$

The entries $\log|U_\omega|$ can take two different values depending on whether site ω is laminar or turbulent: $\log|U_\omega| = \log(1-\varepsilon)$ if $1 \le x_\omega \le r/2$; otherwise, $\log|U_\omega| = \log(1-\varepsilon) + \log r$, if $0 \le x_\omega < 1$. Suppose that there are NF_t turbulent sites in the graph $\mathbb{G}(N, k)$ induced by Ω at time t. Therefore, $\mathrm{Tr}\left(\log|\mathbb{U}_\omega|\right)_{(\omega,\omega)} = N\log(1-\varepsilon) + NF_t\lambda_0$, where $\lambda_0 = \log r$ is the Liapunov exponent of the uncoupled, single map Eq. (2).

The series $\sum_{s>0}(\mathbb{U}^{-1}\mathbb{C})^s/s$ deserves careful consideration. It is easy to check that

$$\mathbb{U}^{-1}\mathbb{C} = \frac{\varepsilon}{k(1-\varepsilon)}\mathbb{A}_{\omega\omega'}, \tag{21}$$

in which $\mathbb{A}_{\omega\omega'}$ is the 'weighted' adjacency matrix of the random graph $\mathbb{G}(N, k)$ such that

$$\mathbb{A}_{\omega\omega'} = \begin{cases} 0, & \omega \text{ and } \omega' \text{ are not coupled,} \\ 1 & \omega \text{ and } \omega' \text{ are in the same state,} \\ r & \omega \text{ is turbulent, } \omega' \text{ is laminar,} \\ 1/r & \omega \text{ is laminar, } \omega' \text{ is turbulent.} \end{cases} \tag{22}$$

The matrix $\mathbb{A}_{\omega\omega'}$ contains data of both topological as well as dynamical configurations of the coupled map system defined on $\mathbb{G}(N, k)$. We denote the adjacency matrix of the graph $\mathbb{G}(N, k)$ as A with entries $A_{ij} = 0$ or 1.

The number of cycles in $\mathbb{G}(N, k)$ is of crucial importance. Let us recall that $\mathrm{Tr}(\mathrm{A}^s) = X_s^0$, i.e. the total number of cycles of the length $s = \{1, \ldots N\}$ in a graph with the adjacency matrix A [18]. While interested in the number of cycles X_s^0 in the random graph $\mathbb{G}(N, k)$, we note that in the matrix $\mathbb{A}$, for each entry proportional to r contributing in a cycle, there is always present the entry $1/r$ such that they are divided out. Therefore, one can prove that $\mathrm{Tr}(\mathbb{A}^s) = \mathrm{Tr}(\mathrm{A}^s) = X_s^0$. We recall that $X_1^0 = 0$ is the number of loops which are ruled out in our model.

Collecting the results of the present subsection and taking the expression Eq. (19) for the mean turbulent fraction $\langle F\rangle$ together with its formal definition Eq. (3) into account, we arrive

at the equation for the free energy $\mathcal{U}$ of the randomly coupled CM map system,

$$\mathcal{U} = \log(1-\varepsilon) + \lambda_0 \frac{\partial \log Z}{\partial r} - \frac{1}{N}\sum_{s>1}^{N} \frac{1}{s}\left[\frac{\varepsilon}{k(1-\varepsilon)}\right]^s X_s^0, \tag{23}$$

where Z is the partition function Eq. (17).

The first term in the Eq. (23) is irrelevant to either the coupled maps dynamics or the random network topology. The second one is a cumulative contribution from all chaotic configurations allowed $\eta \in M^{\mathrm{s}}_{\Phi,\mathbb{G}}$ which coincide with a given one on the cylinder $\mathbb{L}$. Finally, the third term represents a contribution from the topology of the random network.

Equation (23) can hardly be solved explicitly. Nevertheless, some limiting solutions of (23) can easily be found.

6.2 Transitions to the spatio-temporal intermittency and relaminarization

Transitions to the spatio-temporal intermittency and relaminarization deserve the name of phase transitions since the behavior of the mean turbulent fraction $\langle F\rangle$ close to the critical values of coupling ε_c resembles the behavior of thermodynamical quantities close to a critical point.

For the connectivity $k=2$, the coupled maps defined on either regular lattice, [9], or at random exhibit a scaling behavior $\langle F\rangle \propto (\varepsilon-\varepsilon_c)^\beta$ with some critical exponent β that is typical for a *second order* phase transition. In contrast, the transition between laminar states and turbulence for either the RCMN with $k \geq 4$ or the globally coupled maps, [26], appears as a discontinuous jump in $\langle F\rangle$, a feature associated to *first order* phase transitions.

For a backward transition from turbulence to a uniformly laminar states, the situation is different. For minimal connectivities, in both regular coupled maps with local interactions [9] and randomly coupled maps, such a transition does not occur for any $\varepsilon < 1$. For either globally coupled maps [26], or randomly coupled maps with connectivities around $k = 10$, this transition appears as a discontinuous jump. However, for randomly coupled maps with connectivities $k > 10$, this transition follows a power law behavior in $\langle F\rangle$ with another critical exponent γ. The data convincingly show that the formal analogy with phase transitions occurring in statistical mechanics cannot provide us the complete and adequate classification for "critical" phenomena in the RCMN.

It is quite obvious that in a laminar domain $\mathcal{L}$ of the space of external parameters $\mathbb{D} \equiv \{\varepsilon, k, r\}$, the probability $P(\xi)$ (15) to observe a symbolic chaotic configuration ξ on $\mathcal{L}$ is always $P = 0$ for any ξ. Therefore, one could expect that the potential Eq. (16) over the laminar domain $\mathcal{L}$ is $\mathcal{F}|_{\mathcal{L}} = -\infty$.

When the coupling is small $\varepsilon \ll 1$, the influence of random graph topology vanishes. Therefore, the series term in the r.h.s. of Eq. (23) can be neglected in this case. Since $\mathcal{F} = \mathbb{V}\mathcal{U}$ and the cylinder volume $\mathbb{V}$ is taken to be infinite, one can see that the Gibbs potential becomes

$\mathcal{F} = -\infty$, while

$$\langle F \rangle_{\min} < \frac{|\log(1-\varepsilon_c)|}{\log r}. \tag{24}$$

This expression relates the minimal mean turbulent fraction $\langle F \rangle_{\min}$ which can arise at the onset of intermittency for a given value ε_c.

For ε that is not small, the random topology of the network becomes significant. Instead of (24), one obtains

$$\langle F \rangle_{\min} < \frac{|\log(1-\varepsilon_c)|}{\log r} + \frac{1}{N \log r} \left| \sum_{s>1}^{N} \frac{1}{s^2} \left[\frac{\varepsilon_c}{1-\varepsilon_c} \right]^s X_s^0 \right|. \tag{25}$$

Let us consider the series term in Eq. (23). In a random graph $\mathbb{G}(N,k)$, the numbers of cycles X_s^0 ar the Poisson distributed random variables $\mathrm{Po}(\lambda_s^0)$ with means $\lambda_s^0 = k^s/s$. If the number of vertices N in the graph is very large, one can replace the X_s^0 in (23) by their expectations λ_s^0. Consequently, for N large, one arrives at the following expression

$$\frac{1}{N} \sum_{s>1}^{N} \frac{1}{s^2} \left[\frac{\varepsilon}{1-\varepsilon} \right]^s = \frac{\varepsilon^2}{4N(1-\varepsilon)^2} \cdot F\left([1,2,2],[3,3],\frac{\varepsilon}{1-\varepsilon} \right) \tag{26}$$
$$-\frac{\varepsilon^{N+1}}{N(N+1)^2(1-\varepsilon)^{N+1}} \cdot F\left([1,N+1,N+1],[2+N,2+N],\frac{\varepsilon}{1-\varepsilon} \right),$$

where $F([a],[b],x)$ is the generalized hypergeometric function, in which $[a]$ and $[b]$ are the sets of parameters.

The behavior of the term (26) on the parameter ε strongly depends of the random graph topology at given k. For random graphs with minimal connectivities $k = 2$, the random variables counting the number of small cycles whose length s exceeds some maximal length $s > s_{\max}$ is $X_s^0 = 0$. The quantity $s_{\max}$ cannot exceed the size of the giant component of the random graph $\mathbb{G}(N,k)$, but it is actually much smaller. Hence, the effective summation in the r.h.s. of Eqs. (23) and (25) is up to $s_{\max} \ll N$. The contribution to (23) coming from the term (26) slowly increases with ε as $\varepsilon < 1/2$, enhancing the critical value ε_c for the intermittency onset.

The series term (26) plays a crucial role in the transition to a uniformly laminar state. As $k \gg 1$ and $\varepsilon/(1-\varepsilon) \gg 1$, the value of the sum abruptly jumps at some value $\varepsilon > 1/2$ to numbers much larger than N. Therefore, the major contribution to the sum comes from the Hamilton cycles $s = N$. The window of turbulence closes when $\mathcal{U} < 0$.

We conclude this subsection with the notion that no turbulent window would appear in the system for $k \geq 100$. In previous sections, we have shown that for connectivity values $k \gg 1$, the relevant random graph $\mathbb{G}(N,k)$ has no isolated vertices, i.e. for every ordered pair of vertices ω_i and ω_j there is a path in $\mathbb{G}(N,k)$ starting in ω_i and terminating at ω_j. Following the traditional terminology, we shall call such a graph as *irreducible*. Consequently, the adjacency matrix A of the irreducible graph satisfies the following property: for each pair of indices (i,j) there exists some $n \geq 0$ such that $A_{ij}^n > 0$ [18]. The typical length of the shortest path between two arbitrary vertices in an irreducible random graph is $d_{\omega_i \omega_j} = \log N / \log k$ [28].

Let us consider the adjacency matrix A of the graph irreducible $\mathbb{G}(N,k)$. Define a *period* p_ω of a node $\omega \in \Omega$ as the greatest common devisor of those integers $n \in \mathbb{N}$ for which $(\mathrm{A}^n)_{\omega\omega} > 0$. Then the period p_{A} of the matrix is the greatest common divisor of the numbers p_ω, $\omega \in \Omega$, [18]. It is to be noticed that in the model in question $p_{\mathrm{A}} = 2$, since loops are ruled out. We shall call the nodes ω_i and ω_j as *period equivalent*, if the length of path between them, $d_{\omega_i\omega_j}$ is divisible by p_{A}. One can see that as $k = 100$, for $N = 10^4$, all the nodes of the network are period equivalent and, therefore, synchronized.

6.3 Transitions to collective behavior in RCMN

Within windows of turbulence, the Gibbs states given by the formula (15) are not trivial, and the Gibbs potential $\mathcal{F}$ remains finite. A phase transition to the collective behavior occurs in the system of coupled maps in the thermodynamic limit $N \to \infty$ when the Gibbs state (15) is not unique, i.e. there are several (at least two) different Gibbs states with respect to the potential $\mathcal{F}$ defined on symbolic configurations in M^s_Φ.

In the context of the thermodynamic formalism applied to CML, this idea has been proposed in [38]. For each topologically mixing component of the uniformly hyperbolic subset $K \subseteq M^{\mathrm{s}}_{\Phi,\mathbb{G}}$, there is precisely one asymptotic probability distribution which is called the SRB measure (after Sinai-Ruelle-Bowen) on the attractor. For n-periodic components of K, however, there are n different Gibbs states relevant to n-cycling through the subcomponents.

In this subsection, we demonstrate that, in the thermodynamic limit $N \to \infty$, the Gibbs potential and consequently the free energy function are multivalued functions as $\varepsilon > 1/2$.

Let us compute the sum in the r.h.s. of the Eq. (23) as $N \to \infty$. In this case, one obtains

$$\lim_{N\to\infty} \sum_{s>1}^{N} \frac{1}{s}\left[\frac{\varepsilon}{k(1-\varepsilon)}\right]^s X_s^0 = \mathrm{Polylog}\left(2, \frac{\varepsilon}{1-\varepsilon}\right) - \frac{\varepsilon}{1-\varepsilon}, \tag{27}$$

where $\mathrm{Polylog}(2,\alpha)$ is the polylogarithm function.

The point $\varepsilon = 1/2$ is a branch point for all branches of the polylogarithm function. The branch cut can be taken to be the interval $(1,\infty)$. The point $\varepsilon = 0$ is also a branch point, and the branch cut is taken to be the negative real axis. The principal branch is given on the unit disk by the series

$$\mathrm{Polylog}(2,\alpha) = \sum_{k=1}^{\infty} \frac{\alpha^k}{k^2},$$

and there is the general formula for the $(n,m)-$th branch of $\mathrm{Polylog}(2,\alpha)$,

$$\mathrm{Polylog}(2,\alpha) + 2i\pi n \log(\alpha) - 4\pi^2 nm, \quad n,m \in \mathbb{Z},$$

where $\log(\alpha)$ means the principal branch of the logarithm [40].

If we now introduce the result (27) into Eq. (23) and neglect terms $O(1/N)$ as $N \to \infty$, we arrive at the expression

$$\mathcal{U}_{y,m} = \log(1-\varepsilon) + \lambda_0 \frac{\partial \log Z}{\partial r} - 4\pi^2 ym - 2\pi yi \log\left(\frac{\varepsilon}{1-\varepsilon}\right) + \mathrm{O}\left(\frac{1}{N}\right), \tag{28}$$

which reveals the two-parameters set of branches for the free energy function $\mathcal{U}$. Here, we have introduced $m \in \mathbb{Z}$, and $y \equiv n/N \in \mathbb{R}$ as $N \to \infty$. The discrete parameter m enumerates different bands of possible solutions of the Eq. (23), and the parameter y (continuous in the thermodynamic limit) enumerates the different branches of $\mathcal{U}$ within a band. The behavior prescribed by Eq. (28) is clearly seen on Figs. (6) and (7).

6.4 The bifurcation route to collective periodic behavior in RCMN

The graphs presented on Figs. (6) and (7) essentially resemble the "bifurcation diagrams" well known in deterministic chaotic dynamics of unimodal maps over the interval $I = [0,1]$ having a negative Schwarzian derivative.

Consider the irreducible random graph $\mathbb{G}(N,k)$ and its adjacency matrix A. The Perron-Frobenius theory is applied completely to such an irreducible matrix. As a particular consequence of this theory concerning the collective behavior in the RCMN, one can prove that there exist two stable fixed points for the map $\Psi : F_t \to F_{t+1}$ correspondent to either the uniformly synchronized laminar state or to the sustained fully turbulent state of network. Close to these fixed points, a map for the instantaneous turbulent fraction Ψ is a polynomial map in F_t. Therefore, in the unite interval $I = [0,1]$ it turns to be a unimodal function having the negative Schwarzian derivative over the whole interval,

$$\mathcal{S}\Psi \equiv \frac{\Psi'''}{\Psi'} - \frac{3}{2}\left(\frac{\Psi''}{\Psi'}\right)^2 < 0. \tag{29}$$

In this case, Ψ displays an infinite sequence of pitchfork bifurcations when the attractor relevant to the unique Gibbs state losses its stability. An example of such a map has been presented in [26]. These bifurcations are actually observable in some intervals of the parameter values.

In the diagrams shown on Figs. 6 and 7, the bifurcation branches which draw away from the stable point $F_t = 1$ terminate soon, while for the branches which tend to the fixed point where the map Ψ is still polynomial, the consequent pitchfork bifurcations are still observable up to the very end of the turbulent window.

7 Conclusion

In this article we have studied the main features associated with transitions to spatiotemporal intermittency and relaminarization, as well as transitions to collective behavior occurring in randomly coupled Chaté-Manneville minimal maps. Numerical simulations as well as a theoretical framework for these systems have been presented. We have reviewed and classified previous studies devoted to randomly coupled maps networks according to the random graphs spanning the networks. We have studied the probabilistic geometrical properties of the $k-$out model random graphs $\mathbb{G}(N,k)$. The thermodynamic formalism based on the symbolic representation for the dynamics of randomly coupled chaotic maps has been introduced.

We have found that for low connectivity in the network the transition to turbulence via spatiotemporal intermittency in randomly coupled chaotic maps occurs as a power law close to a critical value of the coupling. In contrast, a discontinuous jump in the mean turbulent fraction $\langle F \rangle$ takes place for medium and large connectivities. Previous studies of Chaté-Manneville maps diffusively coupled on regular lattices [12, 19] and on dterminsitic fractal lattices [22] have shown that $\langle F \rangle$ exhibits a scaling behavior close to the critical coupling. On the other hand, $\langle F \rangle$ displays a discontinuous transition if these maps are globally coupled [26].

As the connectivity increases, a synchronization of the system towards the uniformly laminar state occurs at another critical value of the coupling $\varepsilon_c' > \varepsilon_c$. Similarly to the case of globally coupled Chaté-Manneville maps [26], windows of turbulence are established. The onset of re-laminarization appears as a discontinuous jump to a uniformly laminar state if the connectivity is around $k = 10$, and as a power law decay of the mean turbulent fraction $\langle F \rangle$ close to ε_c' for $k > 10$. We have shown that the turbulent windows contracts with increasing connectivity k, until they vanish for $k \geq 100$. Additionally, periodic collective behavior arises within the windows of turbulence, as in globally coupled maps.

Although randomly coupled maps and globally coupled maps have different topological properties, our results show that these two classes of networks behave collectively in analogous ways. Discontinuous phase transitions, well defined turbulent windows and nontrivial collective behavior are common and distinctive features emerging in both classes of networks. The recent observations of dynamical clustering in a randomly coupled map lattice [11], which are commonly seen is globally coupled maps, also contribute to support the idea of the equivalence of both kinds of networks at a global level.

The observed collective properties of the system have been analyzed through the thermodynamic formalism. We have considered the Gibbs potential and the free energy function for the system of randomly coupled maps and derive a closed equation for them. Some properties of the solutions for this equation have been analyzed. In particular, it has been proved that in some interval of the system parameters (i.e., coupling, connectivity, and the local parameter of the Chaté-Manneville map) the Gibbs potential together with the free energy function acquires a two-parameter set of branches. The non-uniqueness of the Gibbs state with respect to the given potential in fact predicts a complex collective periodic behavior.

Acknowledgements

The authors are grateful to the participants of seminars in the Zentrum für Interdisziplinäre Forschung, Universität Bielefeld, especially to R. Lima and A. Pikovsky for illuminating discussions. This work has been performed in connection to the international research project "The Sciences of Complexity: From Mathematics to technology to a Sustainable World", Zentrum für Interdisziplinäre Forschung (ZIF), Universität Bielefeld. One of the authors (D.V.) has been supported by the Alexander von Humboldt Foundation (Germany). S. Sequeira has

been supported by Graduiertenkolleg Strukturbildungsprozesse, Forschungsschwerpunkt Mathematisierung Strukturbildungprocesse, Universiy of Bielefeld (Germany). M.G.C. acknowledges support from the Consejo de Desarrollo Cientifico, Humanistico y Tecnológico at Universidad de Los Andes (Venezuela).

References

[1] K. Kaneko, Progr. Theor. Phys. **72** 480 (1984); **74** 1033 (1985).

[2] K. Kaneko, Physica D **23**, 436-447 (1986).

[3] K. Kaneko, Physica D **41**, 137 (1990).

[4] S. Wasserman, K. Faust, *Social Network Analysis*, Cambridge U. Press, Cambridge (1994).

[5] R. T. Paine, Nature **355**, 73 (1992), K. McCann, A. Hastings, and G. R. Huxel, Nature **395**, 794 (1998).

[6] R. Albert, H. Jeong, and A.-L. Barabási, Nature **401**, 130 (1999), B. A Huberman, L. A. Adamic, Nature **401**, 131 (1999).

[7] M. G. Cosenza, R. Kapral, Phys. Rev. A **46**, 1850 (1992).

[8] P.M. Gade, H. A. Cerdeira, and R. Ramaswamy, Phys. Rev. E **52**, 2478 (1995).

[9] H. Chaté, P. Manneville, Chaos **2**, 307 (1992).

[10] P. Gade, Phys. Rev. E **54**, 64 (1996).

[11] S. C. Manrubia and A. S. Mikhailov, Phys. Rev. E **60**, 1579 (1999).

[12] H. Chaté, P. Manneville, Physica D **32**, 409 (1988).

[13] P. Erdös and A. Rényi, Publicationes Mathematicae **6**, 290 (1959).

[14] B. Ballobás, *Random Graphs*, Academic Press, NY (1985).

[15] S. Janson, T. Łuszak, A. Rucinski, *Random Graphs*, John Wiley & Sons, NY (2000).

[16] V. F. Kolchin, *Random Mappings*, Optimization Software, NY (1986).

[17] D. J. Aldous, J. Pitman, Random Structures Algorithms **5**, 487 (1994).

[18] D. Lind, B. Marcus, *An Introduction to Symbolic Dynamics and Coding*, Cambridge Univ. Press., Cambridge (1995).

[19] H. Chaté and P. Manneville, Europhys. Lett. **6**, 591 (1988).

[20] K. Kaneko, Prog. Theor. Phys. **74**, 1033 (1985).

[21] D. Stassinopoulos and P. Alstrøm, Phys. Rev. A **45**, 675 (1992).

[22] M. G. Cosenza, R. Kapral, Chaos **4**, 99 (1994).

[23] M. G. Cosenza and K. Tucci, Chaos, Solitons and Fractals **11**, 2039 (2000).

[24] P. Grassberger, T. Schreiber, Physica D **50**, 177 (1991).

[25] J. M. Houlrik, I. Webman, M. H. Jensen, Phys. Rev. A **41**, 4210 (1990).

[26] M. G. Cosenza, A. Parravano, Phys. Rev. E **53**, 6032 (1996).

[27] H. Chaté and P. Manneville, Prog. Theor. Phys. **87**, 1 (1992).

[28] M. E. J. Newman, S. H. Strogatz, and D. J. Watts, EPrint arXiv: Random graphs with arbitrary degree distribution and their applications, cond-mat/0007235 (2000).

[29] P. Erdős, A. Rényi, Publ. Math. Inst. Hungar. Acad. Sci. **5**, 17 (1960).

[30] The falling factorial is

$$(N)_m = N^m \exp\left(-\frac{m^2}{2N} - \frac{m^3}{6N^2} - \mathrm{O}\left(\frac{m}{N} + \frac{m^4}{N^3}\right)\right) \sim N^m,$$

as $N \to \infty$.

[31] E. Friedgut, *Sharp Thresholds of Graph Properties, and the k-sat problem*, J. Amer. Math. Soc. **12**, 1017-1054 (1999).

[32] Sinai Ya., Russ. Math. Surveys **28**, 21 (1972)

[33] D. Ruelle, *Thermodynamic Formalism,* **5** of *Encyclopedia of Mathematics and its Applications* (Addison-Wesley, Reading, Mass., 1978).

[34] M. Jiang, private communication. D.V. is grateful to M. Jiang for this comment.

[35] J. Bricmont, A. Kupiainen, Commun. Math. Phys. **178**, 703 (1996).

[36] M. Jiang, Ya. B. Pesin, Commun. Math. Phys. **193**, 1391 (1998).

[37] H. Chaté, Physica D **86**, 238 (1995).

[38] G. Gielis, R. S. MacKay, Nonlinearity, **13**, 867 (2000).

[39] S. Janson, Combin. Probab. Comput. **4**, 369 (1995).

[40] L. Lewin, *Polylogarithms and Associated Functions*, North Holland, Amsterdam (1981).

Figures

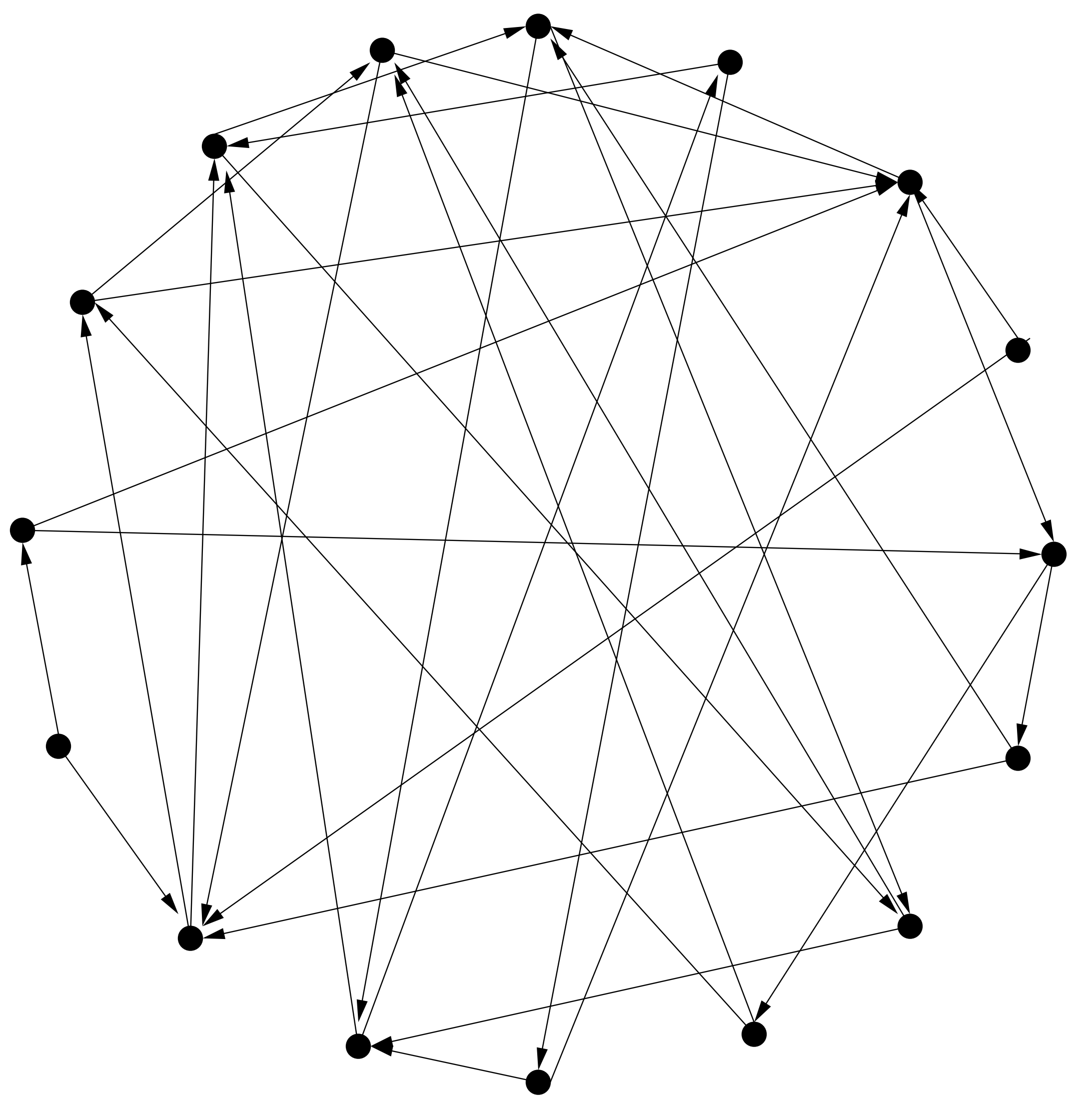

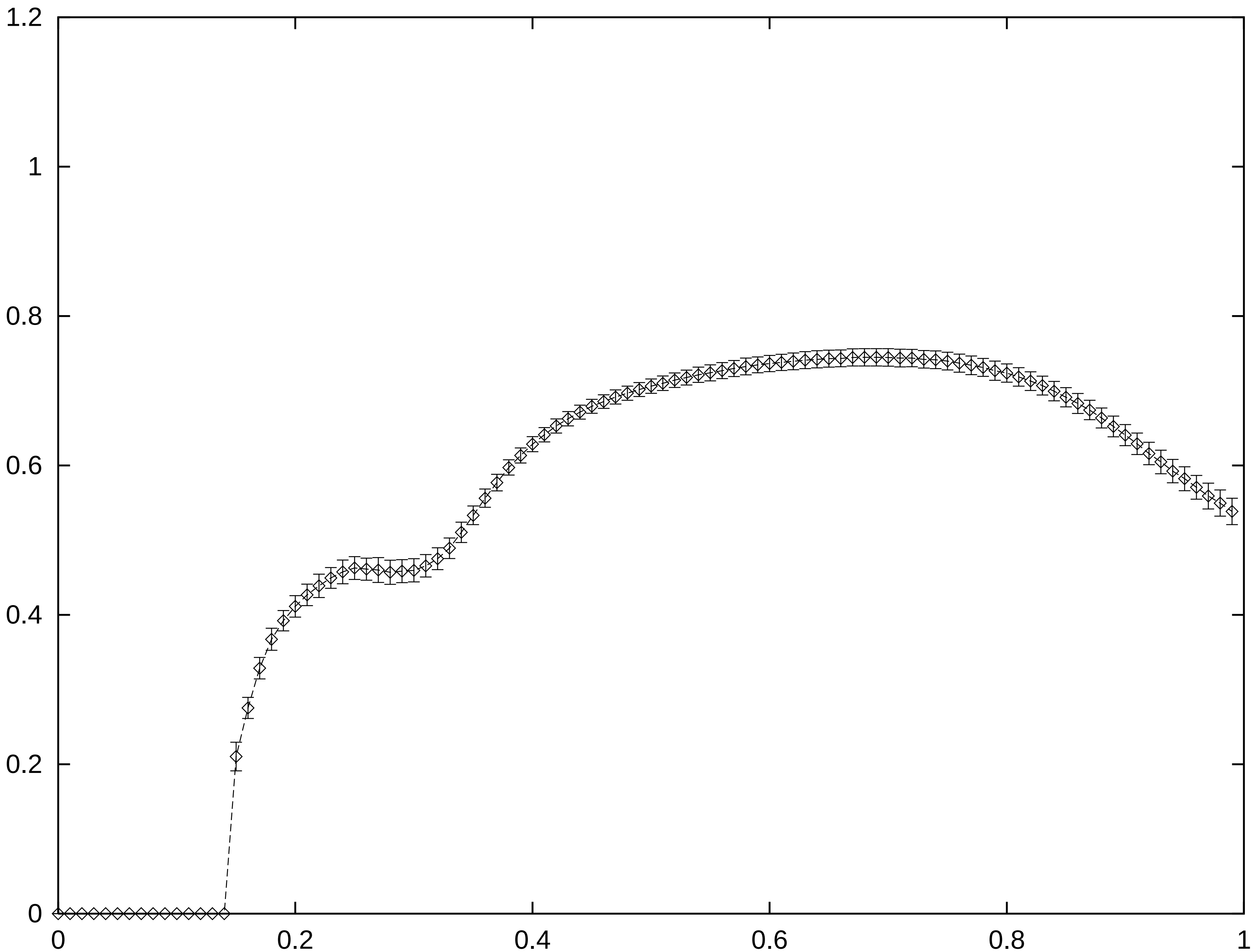
1.2
1
0.8
0.6
0.4
0.2
0
0
0.2
0.4
0.6
0.8
1

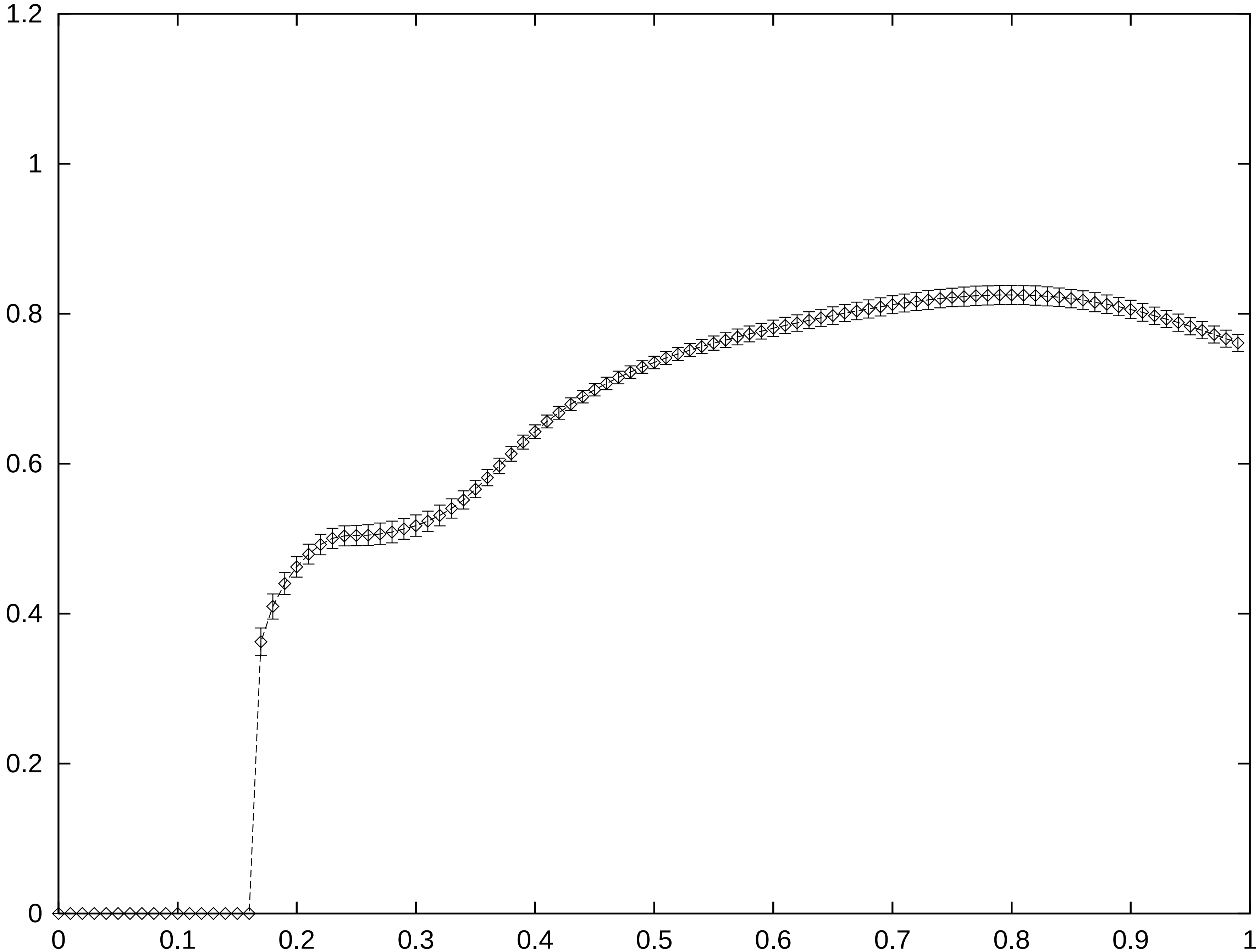
1.2
1
0.8
0.6
0.4
0.2
0
0
0.1
0.2
0.3
0.4
0.5
0.6
0.7
0.8
0.9
1

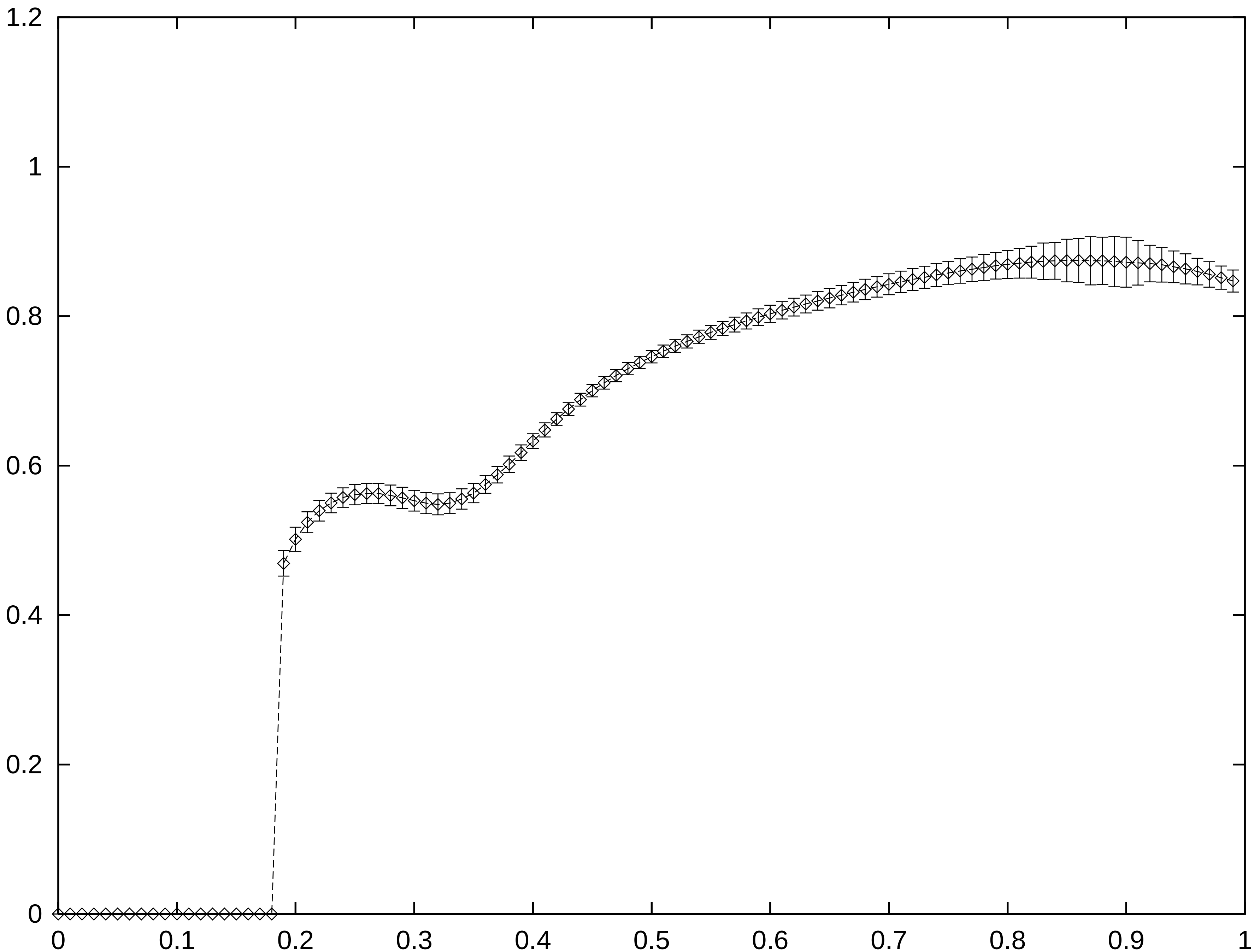
1.2
1
0.8
0.6
0.4
0.2
0
0
0.1
0.2
0.3
0.4
0.5
0.6
0.7
0.8
0.9
1

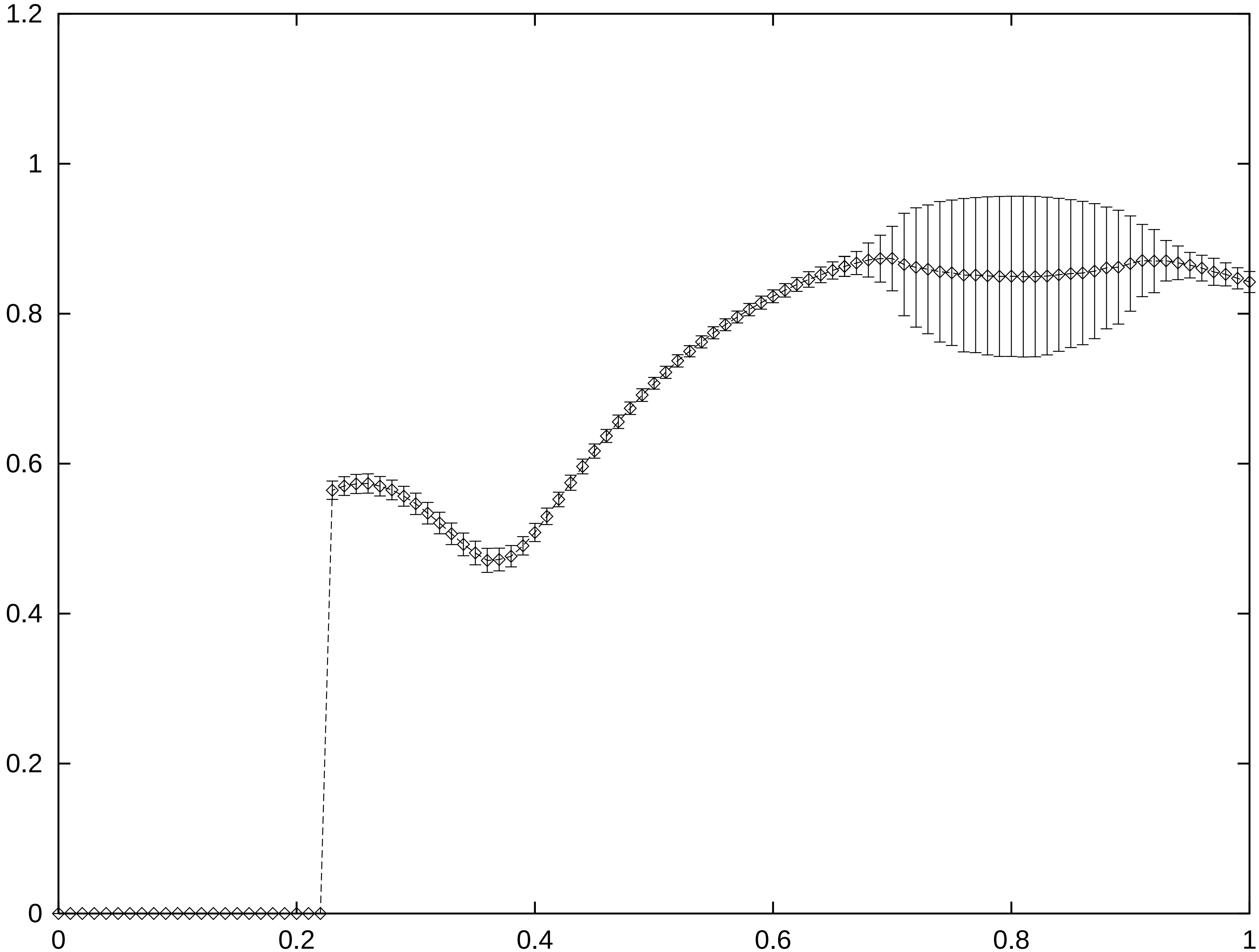

1.2
1
0.8
0.6
0.4
0.2
0
0
0.2
0.4
0.6
0.8
1

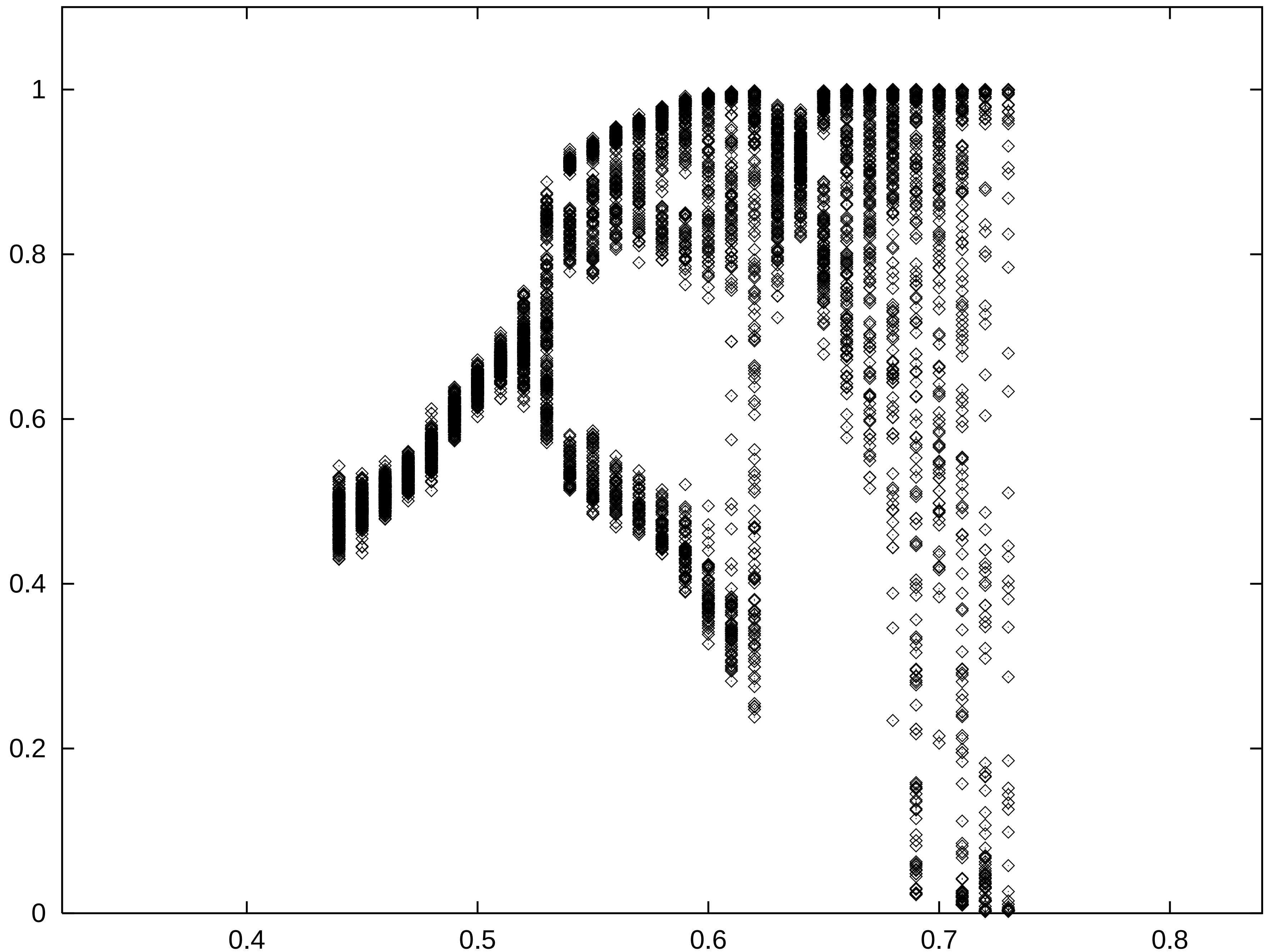

1
0.8
0.6
0.4
0.2
0
0.4
0.5
0.6
0.7
0.8

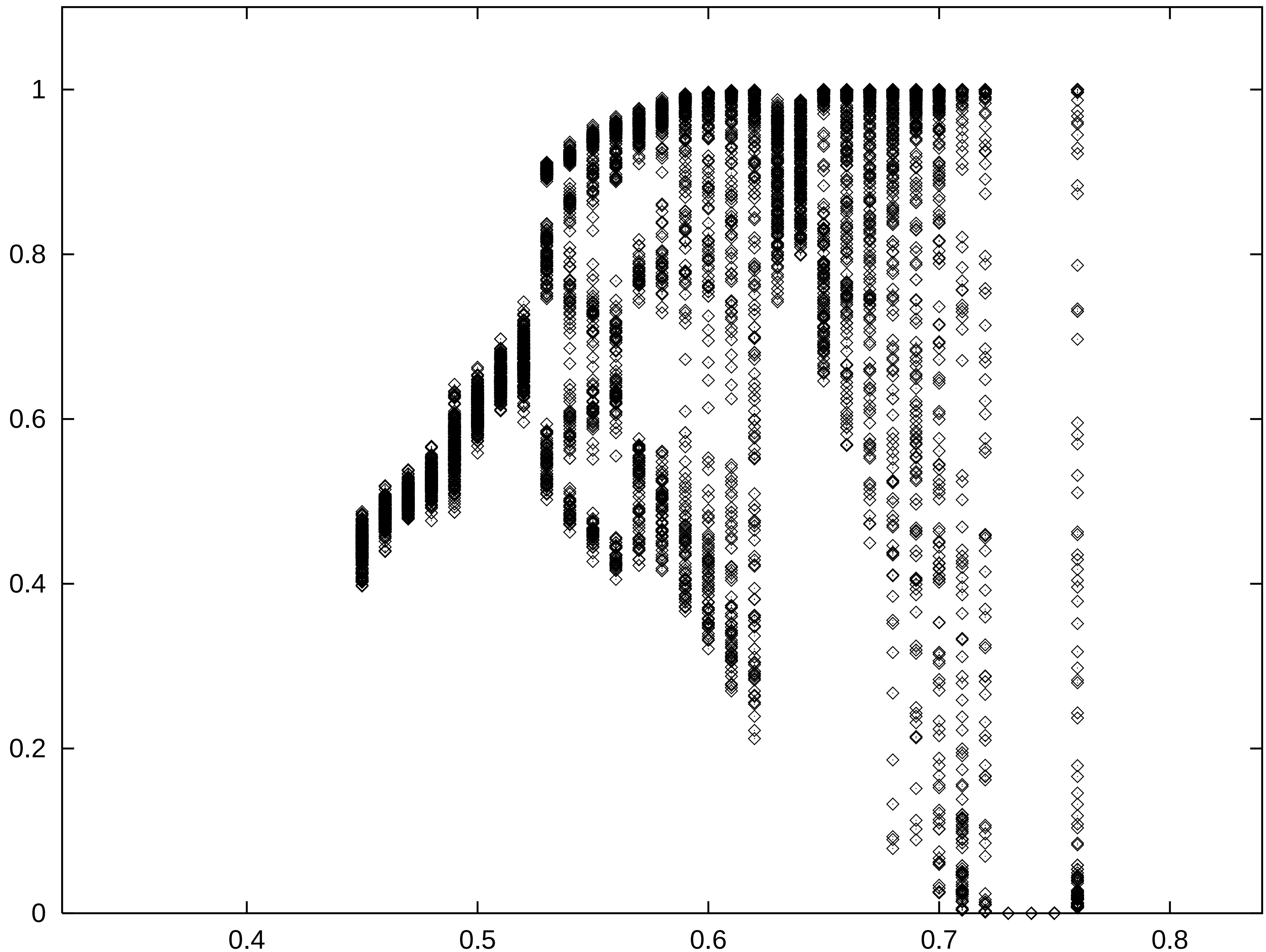

1
0.8
0.6
0.4
0.2
0
0.4
0.5
0.6
0.7
0.8

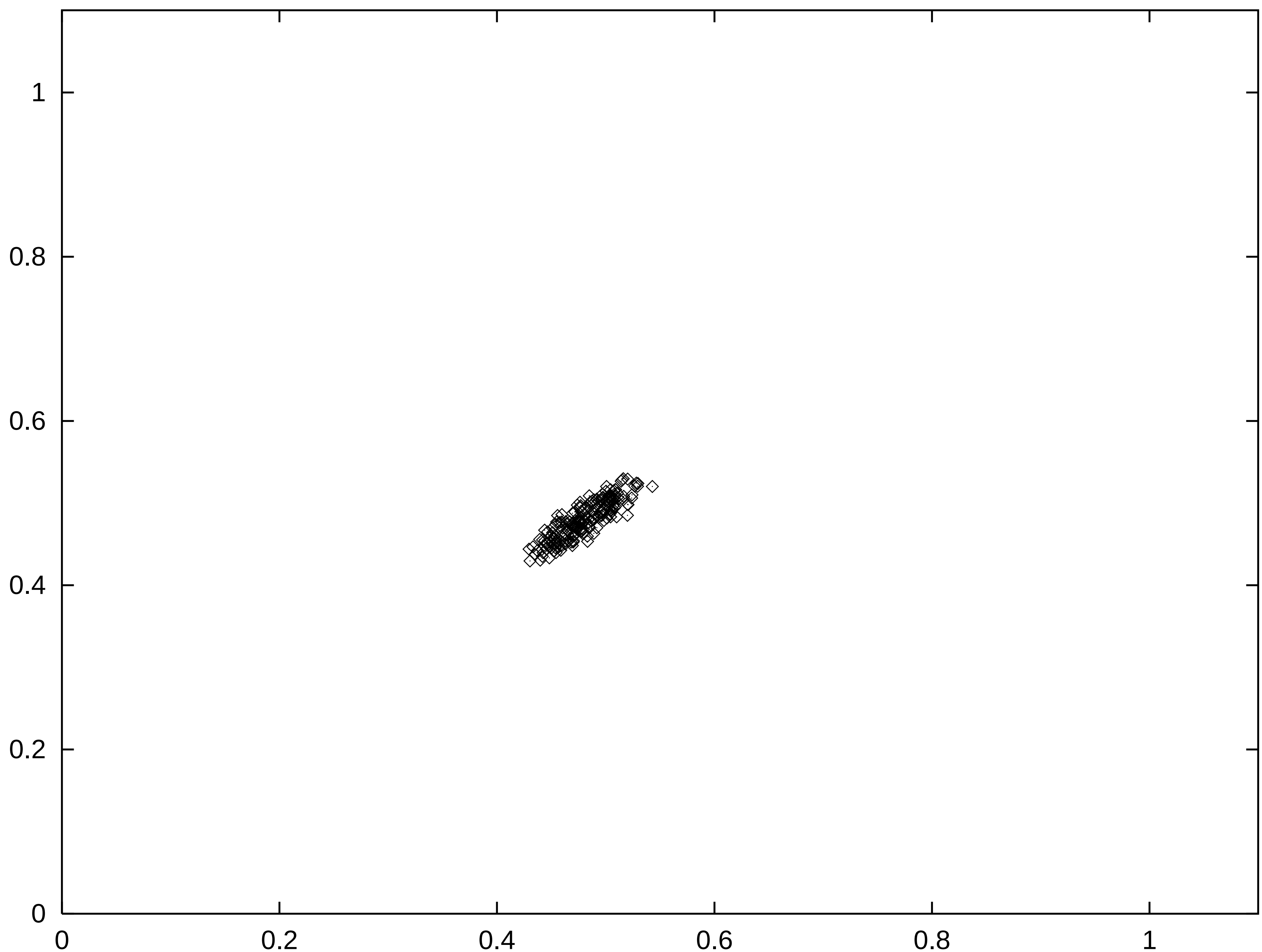
0
0.2
0.4
0.6
0.8
1

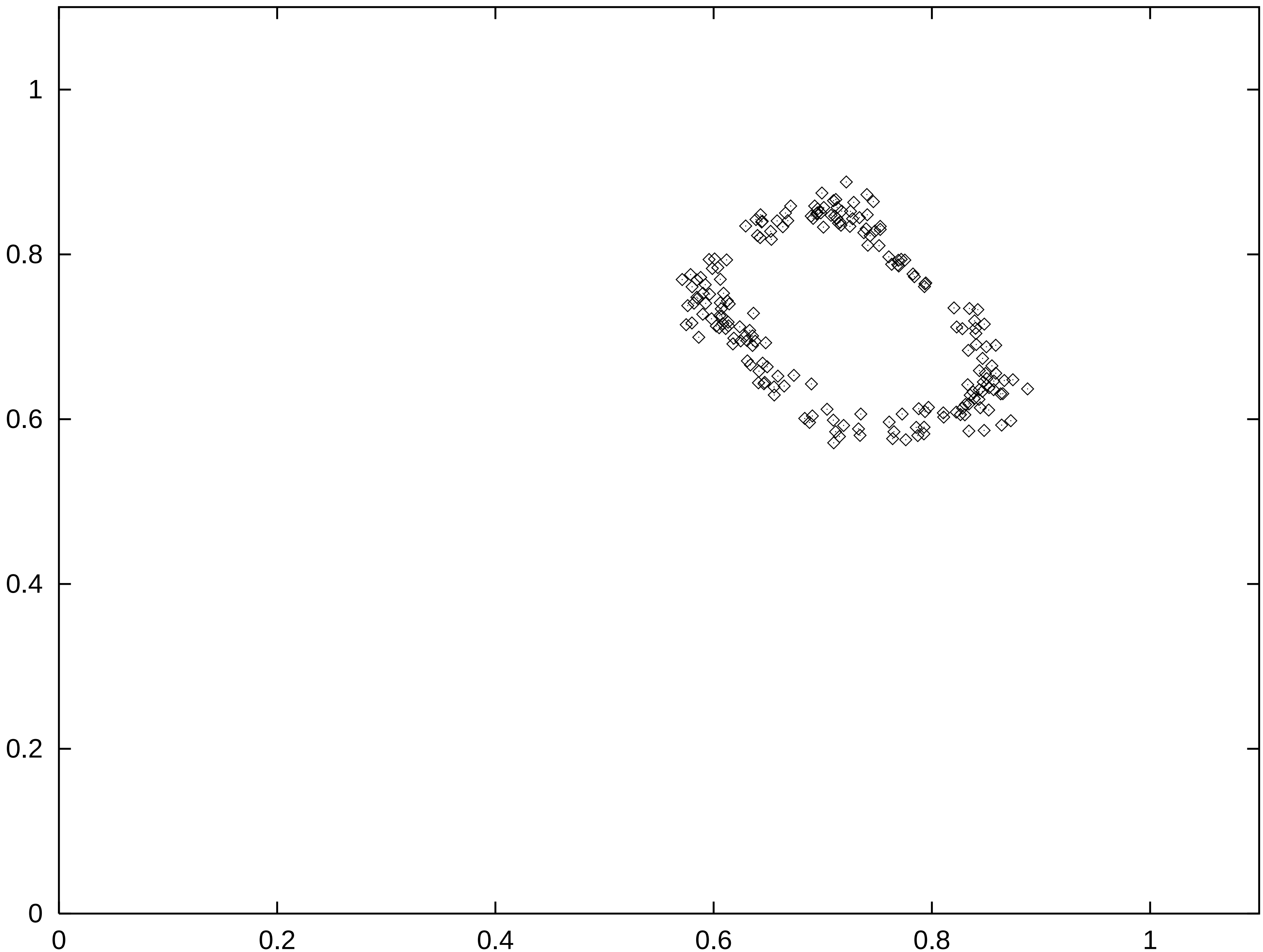
1
0.8
0.6
0.4
0.2
0
0
0.2
0.4
0.6
0.8
1

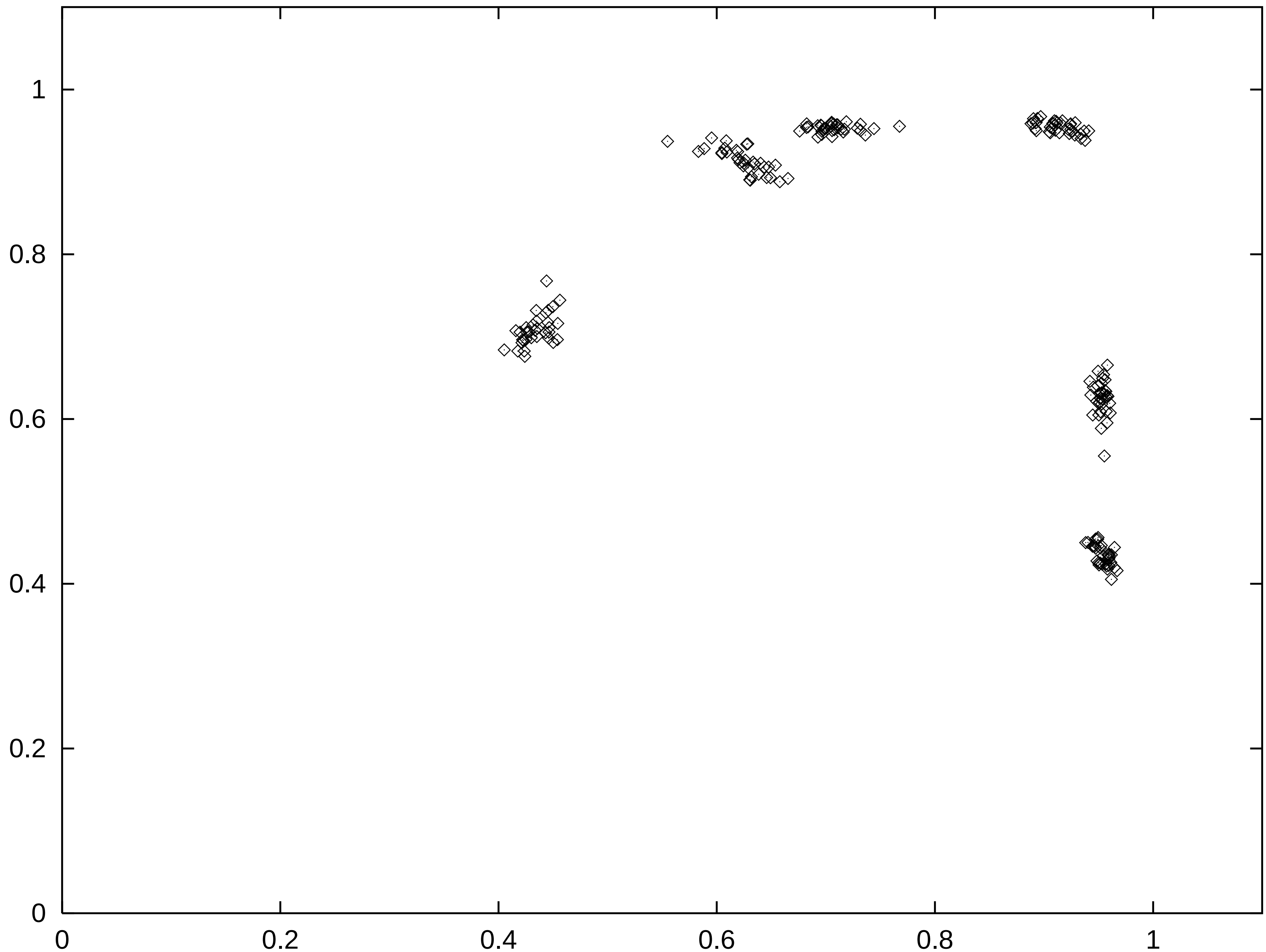

0
0.2
0.4
0.6
0.8
1
0
0.2
0.4
0.6
0.8
1

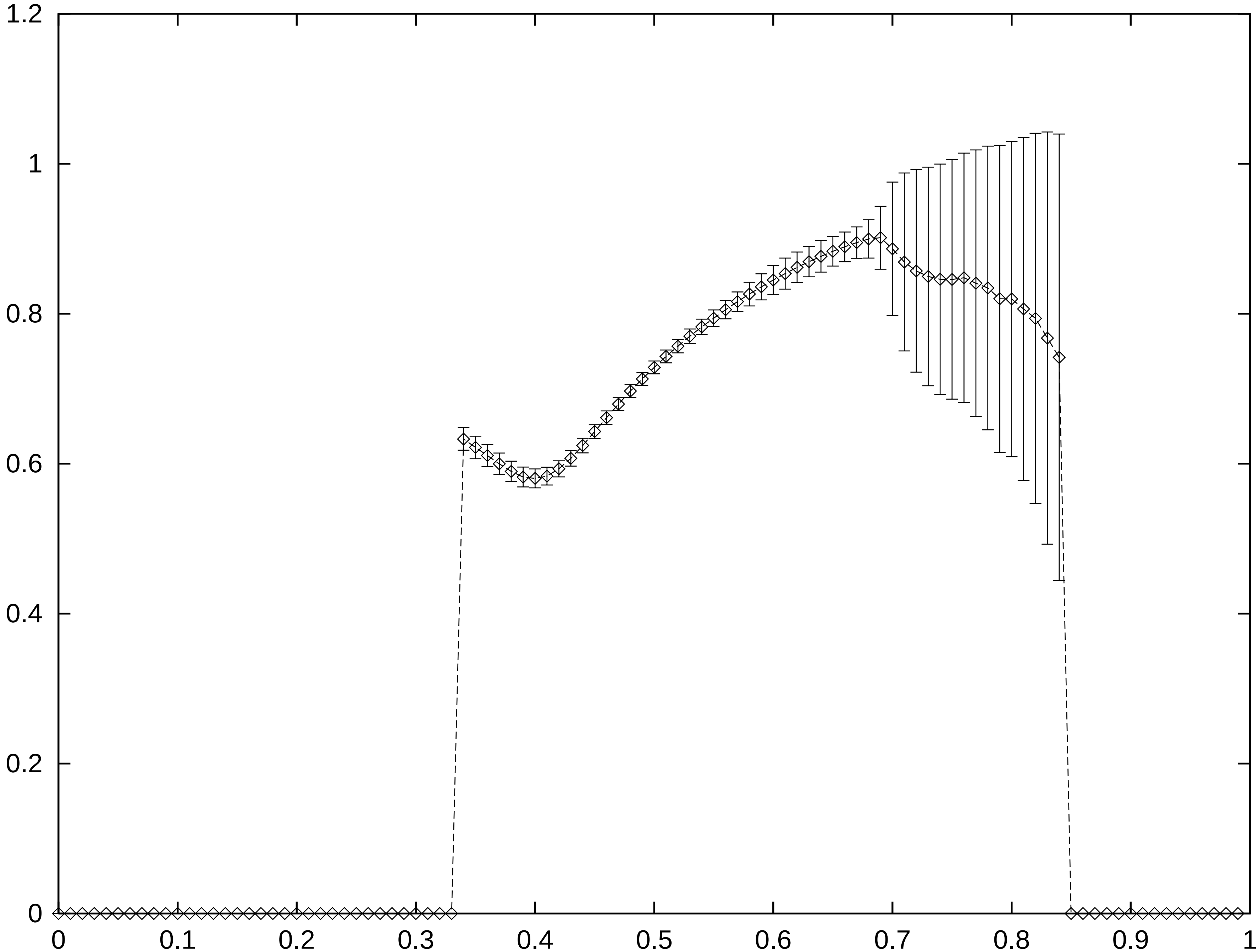
1.2
1
0.8
0.6
0.4
0.2
0
0
0.1
0.2
0.3
0.4
0.5
0.6
0.7
0.8
0.9
1

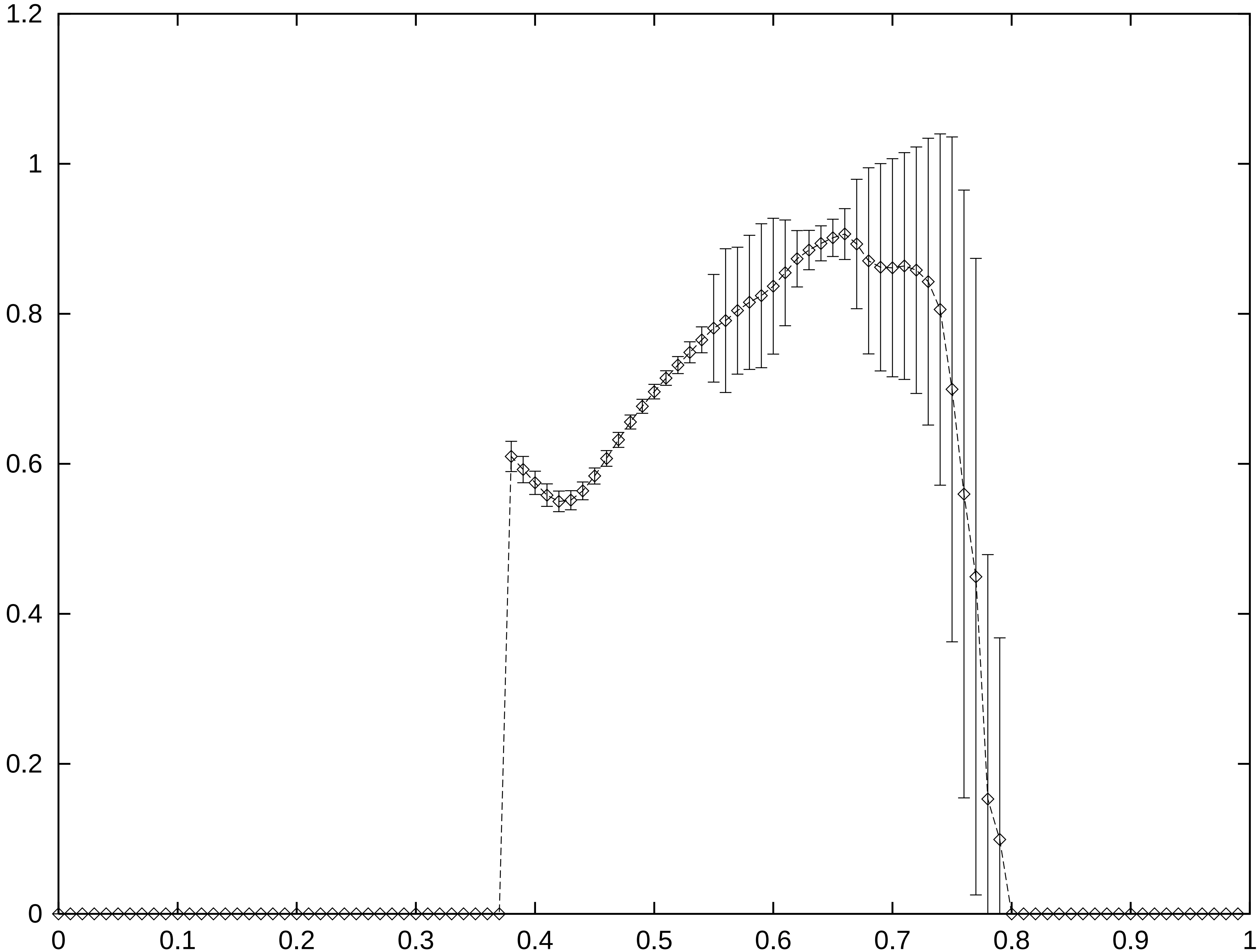

1.2
1
0.8
0.6
0.4
0.2
0
0
0.1
0.2
0.3
0.4
0.5
0.6
0.7
0.8
0.9
1

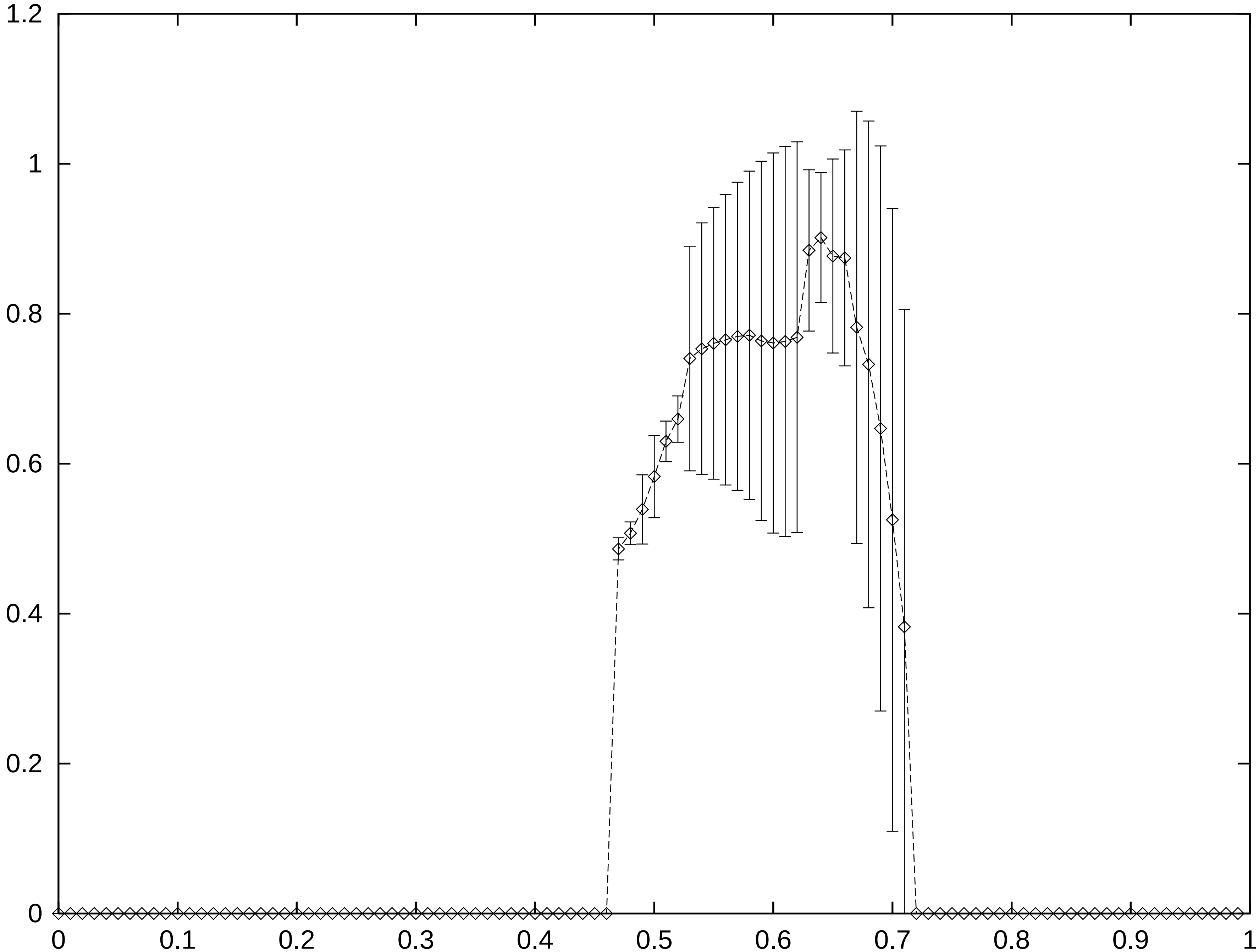

1.2
1
0.8
0.6
0.4
0.2
0
0
0.1
0.2
0.3
0.4
0.5
0.6
0.7
0.8
0.9
1

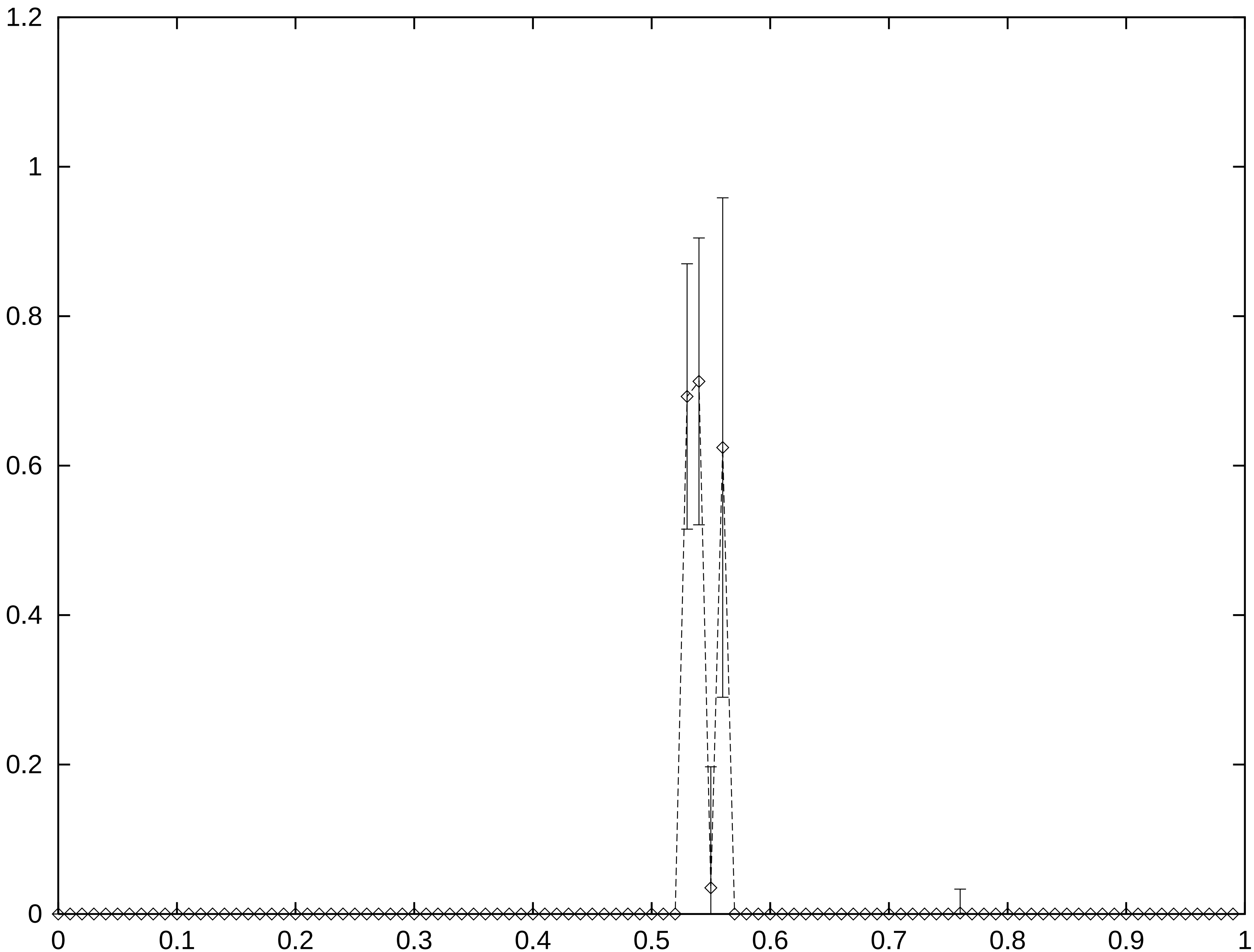
1.2
1
0.8
0.6
0.4
0.2
0
0.1
0.2
0.3
0.4
0.5
0.6
0.7
0.8
0.9
1